4. Stochastic Channel Models

Contents:

4. Stochastic Channel Models

Contents (cont’d):

- WAND model
- Spencer-Jeffs-Jensen-Swindlehurst model
- IEEE 802.11 model
- 3GPP Stochastic Channel Model

The importance of stochastic channel modelling

Main application fields of stochastic channel models:

•*Design and optimization of communication systems:*

- Design of the constituents of communication systems
- Optimization of the behaviour and performance of these constituents
- Analytical or simulation-based investigations of the performance of these constituents

•*Monte Carlo simulations for system performance assessment*

- Link-level simulations (today)
- System-level simulations (today)
- Simulation of cooperative networks (coming soon)

in complex scenarios as close as possible to real operation conditions

Stochastic channel models (SCMs) are crucial and indispensable tools in the design of communication systems.

Radio channel simulation

The different approaches for channel simulations:

- **Stored Channel Models (ATDMA)**

Measured space-variant or time-variant delay spread functions (SFs) are selected according to some specified criteria to form classes of so-called **“reference channels”**. These delay SFs are stored and can be read on demand for simulation purposes.

Example:
Reference space-variant delay SF in an atypical microcellular urban environments:

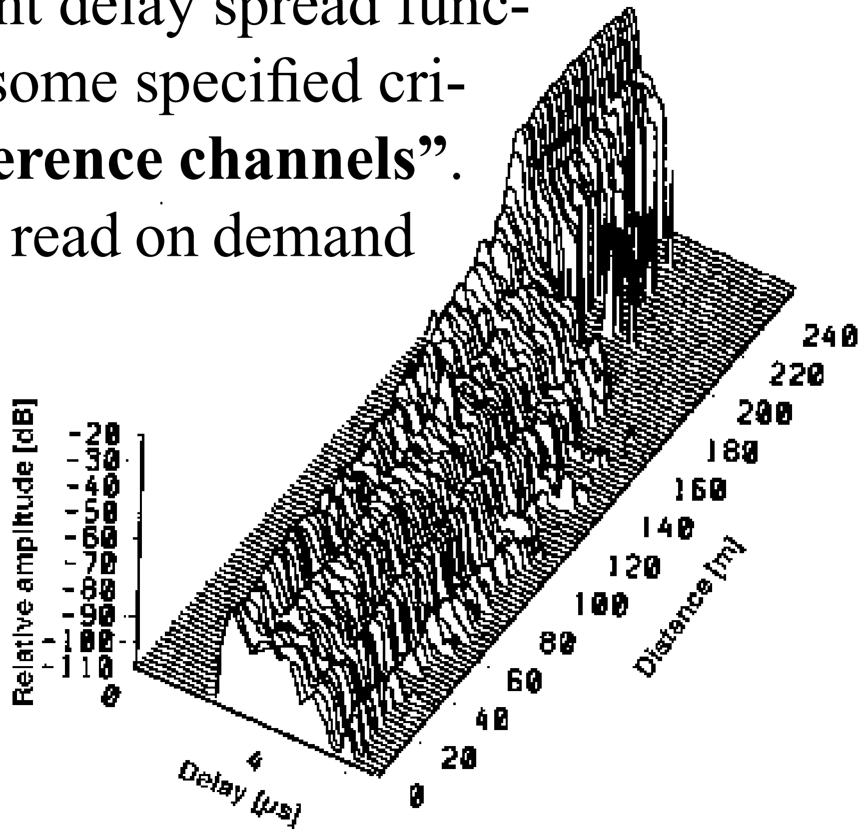

Radio channel simulation

The different approaches for channel simulations (cont'd):

- **Deterministic Channel Models**

  These models employ ray optical techniques (ray tracing, ray launching combined with UTD method) to compute the delay SF or the direction-delay SF using some more or less extensive geographical information (building layout, electric properties of walls and floors, etc.) about the propagation environment under consideration.

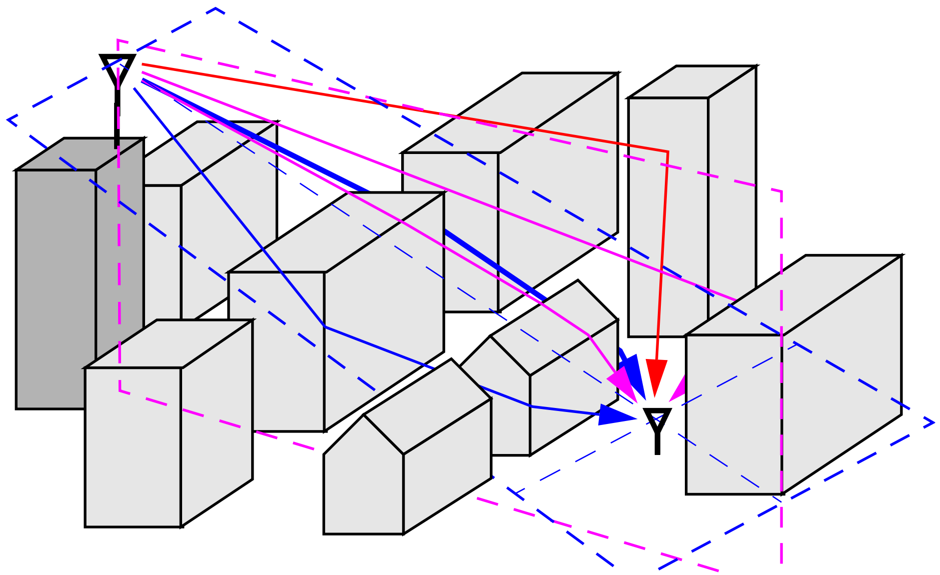

Radio channel simulation

The different approaches for channel simulations (cont'd):

- **Stochastic Channel Models (COST 207, CODIT)**
  - A parametric model for the delay SFs is derived.
  - Realizations of the delay SF are then generated according to specified probability distributions of the model parameters.
  - These probability distributions are gathered by means of statistical analyses of measurement data collected during extensive measurement campaigns.

Example: COST 207 HT

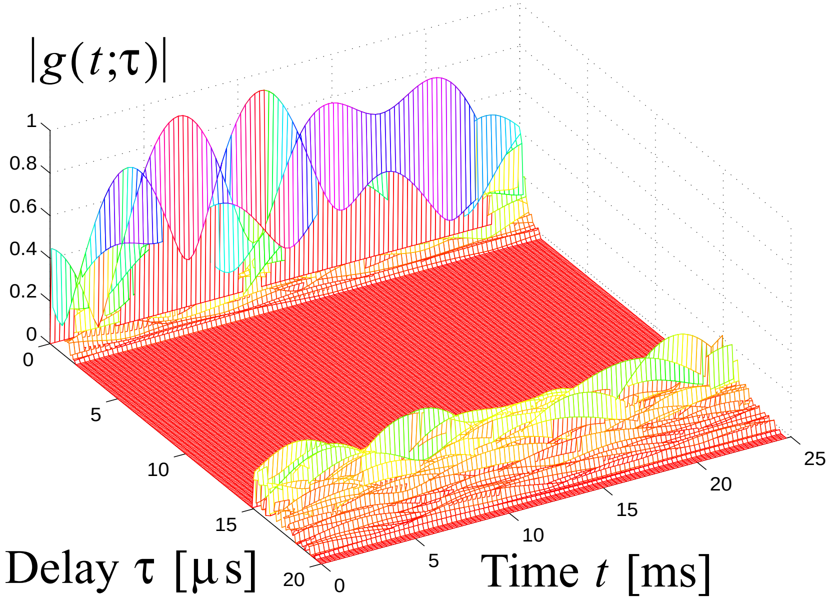

Radio channel simulation

Comparison of the different approaches:

Channel simulation approaches	Computational expense	Intrinsic variability of the models	Retained channel features	Challenge
Reference channels	**High** (storage)	**Low** (=number of stored channels)	**All**	**Choice of the appropriate selection criteria**
Deterministic channel models	**High** (identification of the dominant propagation paths)	**Medium** (=number of environments considered)	**Part of them** (ray optical methods are not exact)	**Identification of the dominant prop. paths + accurate method for computing the path weights**
Stochastic channel models	**Low**	**High** (probability distributions)	**Part of them** (depending on the model used)	**Incorporate all relevant channel features**

Stochastic modelling

Features to be incorporated into SCMs:

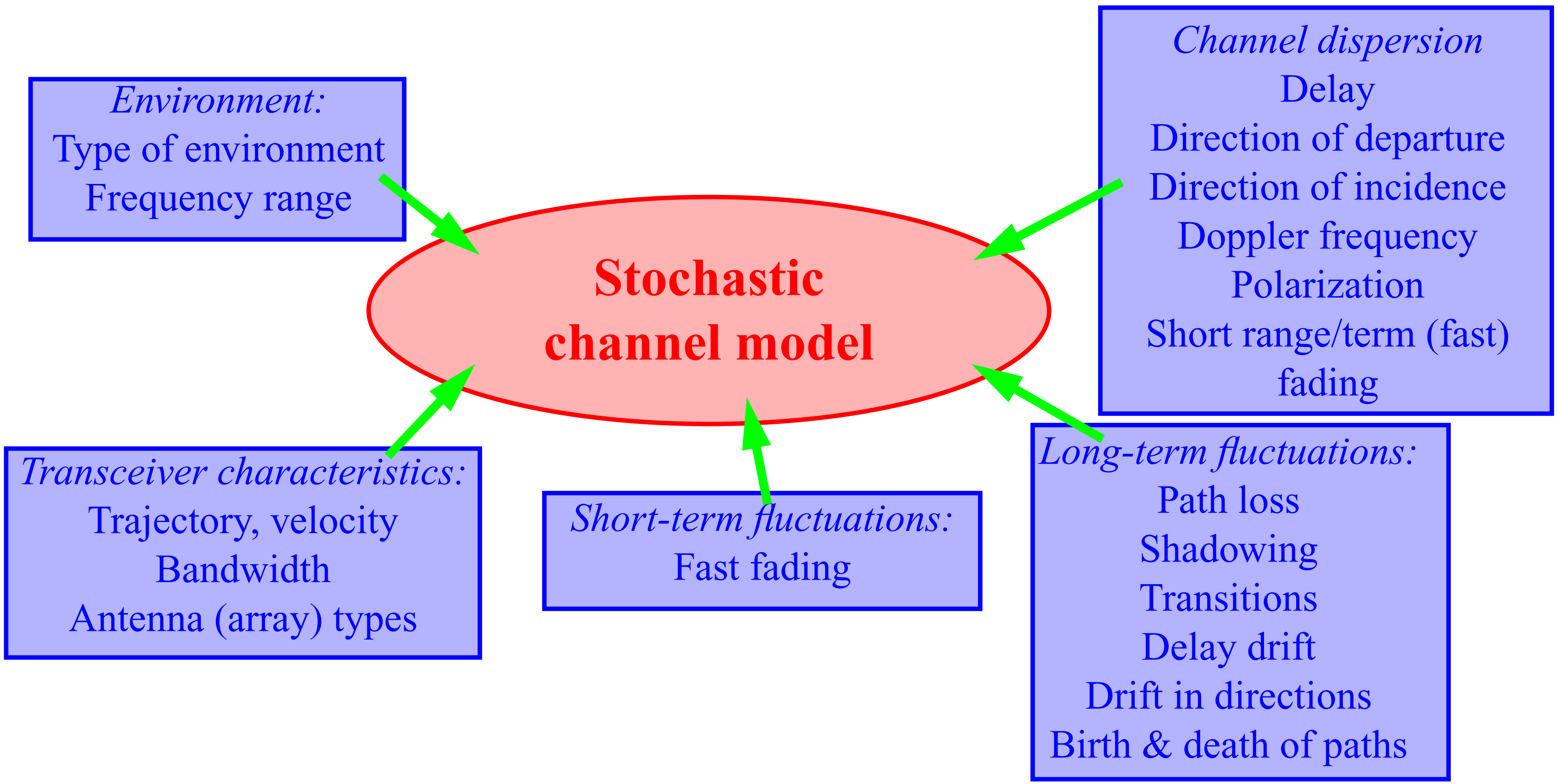

Stochastic modelling

Requirements for SCMs:

- ***Completeness***

  SCMs must reproduce all effects that impact on the performance of communication systems.

  => Guarantee simulation scenarios close to reality
  => Full basis for system comparisons

- ***Accuracy***

  SCMs must accurately describe these effects.

  => Realistic results from analytical and/or simulation-based investigations

- ***Simplicity/low complexity***

  Each effect must be described by a simple model.

  => Enable theoretical study of some particular system aspects and performance
  => Tractable computational effort to simulate the channel in Monte Carlo simulations

Stochastic modelling

Approach for SCM:

Specification of
- the area type
- additional system parameters (array characteristics, mobile velocity, etc.)

Software package generating a specific parametric system function of the channel, e.g.

$$g(t;\tau) \equiv \sum_{i=1}^{N} g_i(t) \cdot \delta(\tau - \tau_i(t))$$

Statistical processing of data obtained from extensive measurement campaigns in the identified areas

Estimation of the probability density functions of the parameters occurring in the parametric system function

Realizations of the system function, e.g. $g(t;\tau)$

Stochastic modelling

Model for $g_i(t)$:

Short-term fluctuations:

$$g_i^{(\mathrm{ST})}(t) = g_{i,c}(t) + g_{i,d}(t)$$

Specular part:

$$g_{i,c}(t) = h_{i,c} \exp(j2\pi\nu_i t)$$

ν_i: Doppler frequency

Diffuse part:

$g_{i,d}(t)$ is a WSS zero-mean circular symmetric complex Gaussian process specified by its ACF $R_i(\Delta t)$ or equivalently its (Doppler) spectrum $P_i(\nu)$:

$$R_i(\Delta t) \;\overset{\Delta t \qquad \nu}{\circ\!\!-\!\!\!-\!\!\!-\!\!\bullet}\; P_i(\nu)$$

Stochastic modelling

Model for $g_i(t)$ (cont'd):

Long-term fluctuations (path loss & shadowing effect):

$$\boxed{g_i(t) = 10^{-\frac{L(t)}{10}} 10^{\frac{\Delta L_i(vt)}{10}} g_i^{(\mathrm{ST})}(t)}$$

- $L(t)$: time-dependent path loss computed from one of the models presented in Lecture 3.
- $\Delta L_i(d)$: real zero-mean Gaussian process with ACF $R_{\Delta L_i}(\Delta d)$.

Usually,

$$\boxed{R_{\Delta L_i}(\Delta d) = \Upsilon^2 \exp(-\Delta d^2 / \kappa^2)}$$

- Υ: standard deviation of $\Delta L_i(d)$
  $\Upsilon = 6 - 8$ dB
- κ: decorrelation length
  Small macrocells: $\kappa = 5 - 8$m

Stochastic modelling

Models for $\tau_i(t)$ **:**

Short-term fluctuations:

$$\boxed{\tau_i(t) = \tau_i}$$

where $\{\tau_1, \tau_2, \ldots, \tau_i, \ldots\}$ is a specified random point process.

Long-term fluctuations:

$$\boxed{\tau_i(t) = \tau_i + \Delta\tau_i(t)}$$

where $\{\tau_1, \tau_2, \ldots, \tau_i, \ldots\}$ is the above random point process and $\{\Delta\tau_i(t)\}$ is a sequence of random processes describing the drift of the components in the time-variant SF on the delay axis.

COST 207 model

Main characteristics:

Cell type	• Macrocell
Area	• Typical non-hilly urban (TU), bad hilly urban (BU) • Non-hilly rural area (RA), hilly terrain (HT)
Frequency range	• Around 1 GHz
Time-variant SF	• $g(t;\tau) = \sqrt{\frac{P}{N}} \sum_{i=1}^{N} \exp\{j(2\pi\nu_i t + \varphi_i)\} \cdot \delta(\tau - \tau_i)$
Input	• Area type • Vehicle velocity • Number of components in $g(t;\tau)$ • Delay and Doppler resolution

COST 207 model

Normalized delay-Doppler scattering function:

$$P_n(\nu, \tau) \equiv \frac{1}{P} P(\nu, \tau) \qquad \left(\Rightarrow \int P_n(\nu, \tau) d\nu d\tau = 1 \right)$$

We can decompose $P_n(\nu, \tau)$ as

$$\boxed{P_n(\nu, \tau) = \underbrace{P_n(\tau)}_{\text{Normalized delay scattering function}} \cdot \underbrace{P_n(\nu|\tau)}_{\text{Delay-dependent normalized Doppler scattering function}}} \qquad \left(P_n(\tau) \equiv \int P_n(\nu, \tau) d\nu\right)$$

The COST 207 models are specified by the two functions:

- $P_n(\tau)$
- $P_n(\nu|\tau)$

COST 207 model

Normalized delay scattering function:

Typical urban non-hilly area (TU):

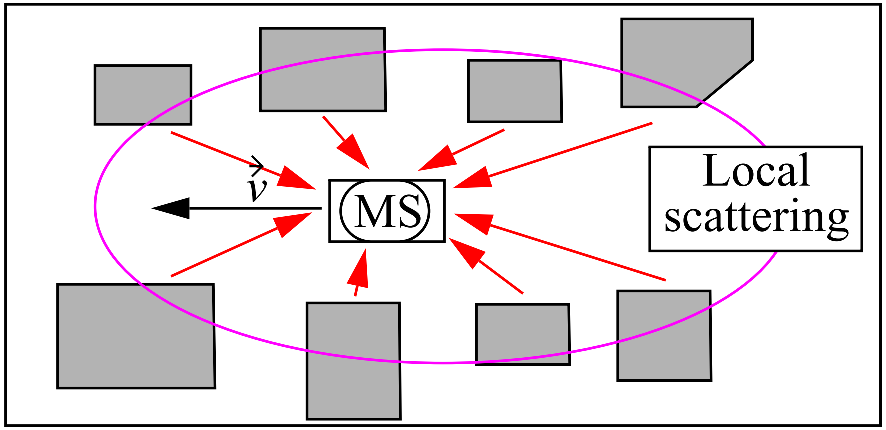

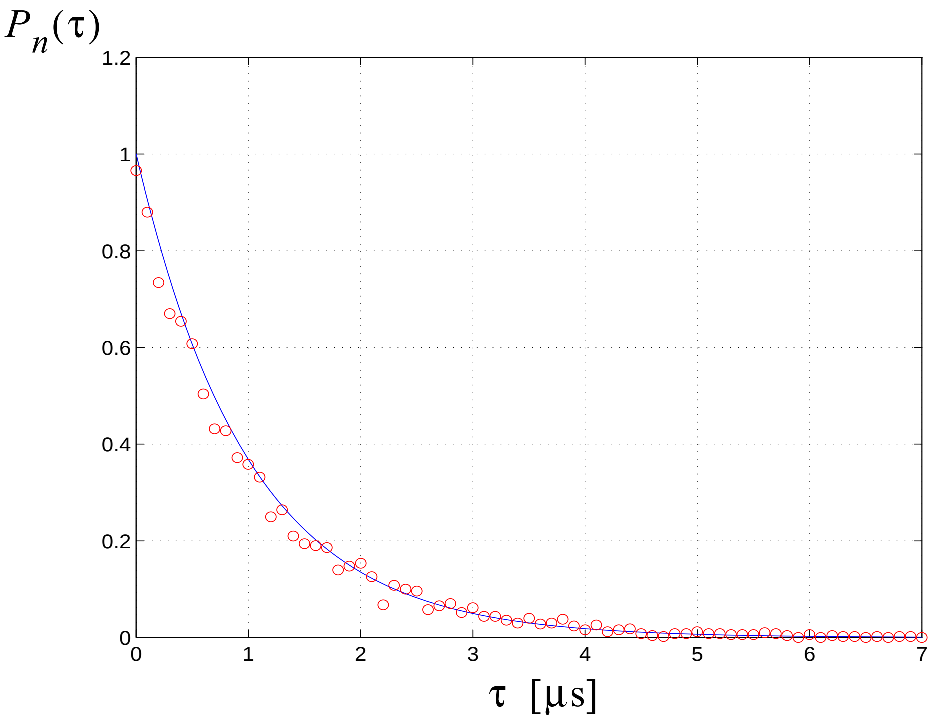

$$P_n(\tau) \propto \begin{cases} \exp(-\tau) \; ; & 0 \le \tau_{[\mu s]} \le 7 \\ 0 \; ; & \text{elsewhere} \end{cases}$$

COST 207 model

Normalized delay scattering function (cont'd):

Typical bad urban hilly area (BU):

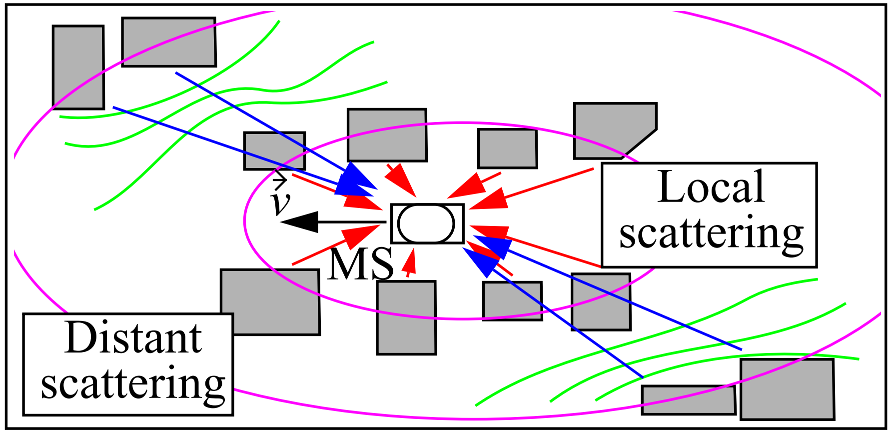

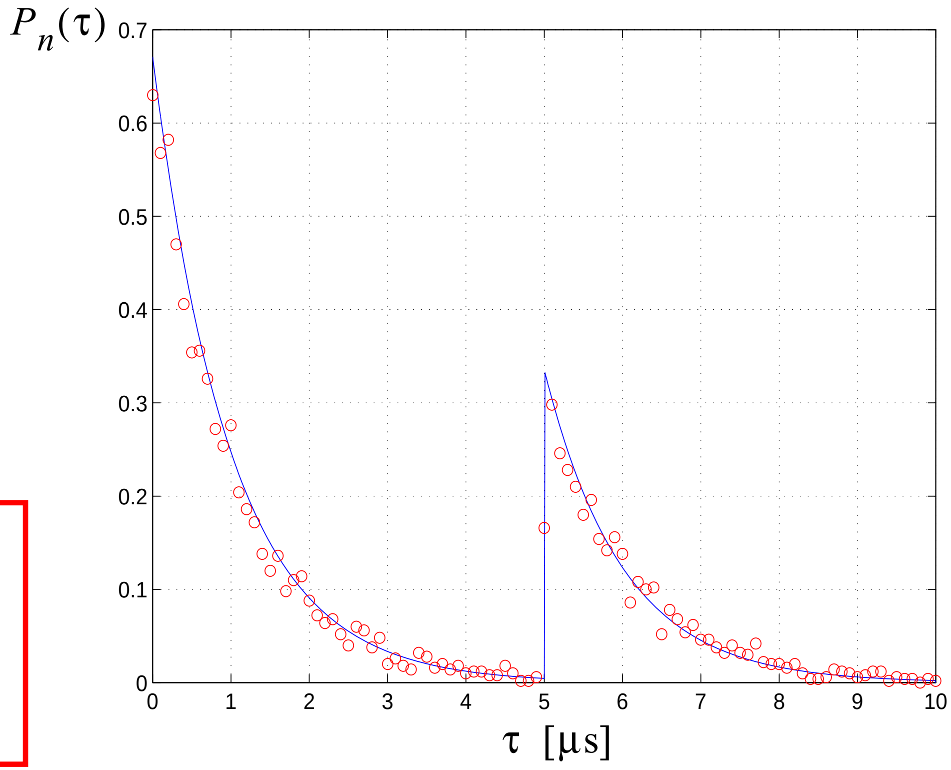

$$P_n(\tau) \propto \begin{cases} \exp(-\tau) & ; \quad 0 \le \tau_{[\mu s]} \le 5 \\ 0.5\exp(5-\tau) & ; \quad 5 \le \tau_{[\mu s]} \le 10 \\ 0 & ; \quad \text{elsewhere} \end{cases}$$

COST 207 model

Normalized delay scattering function (cont'd):

Typical rural non-hilly area (RA):

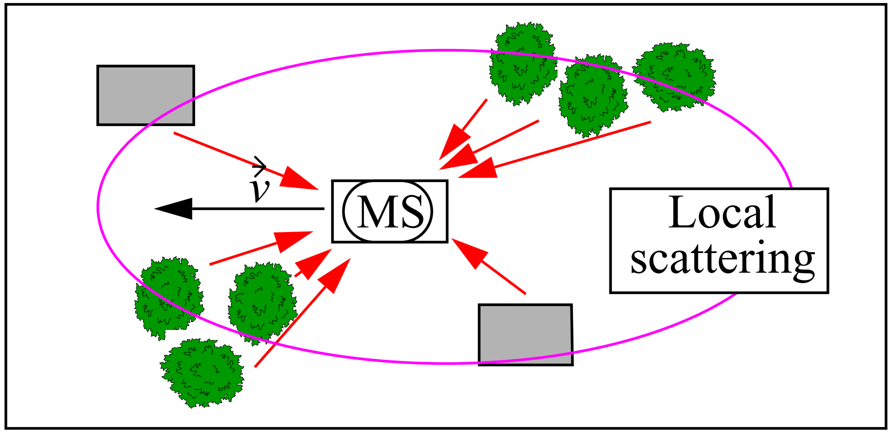

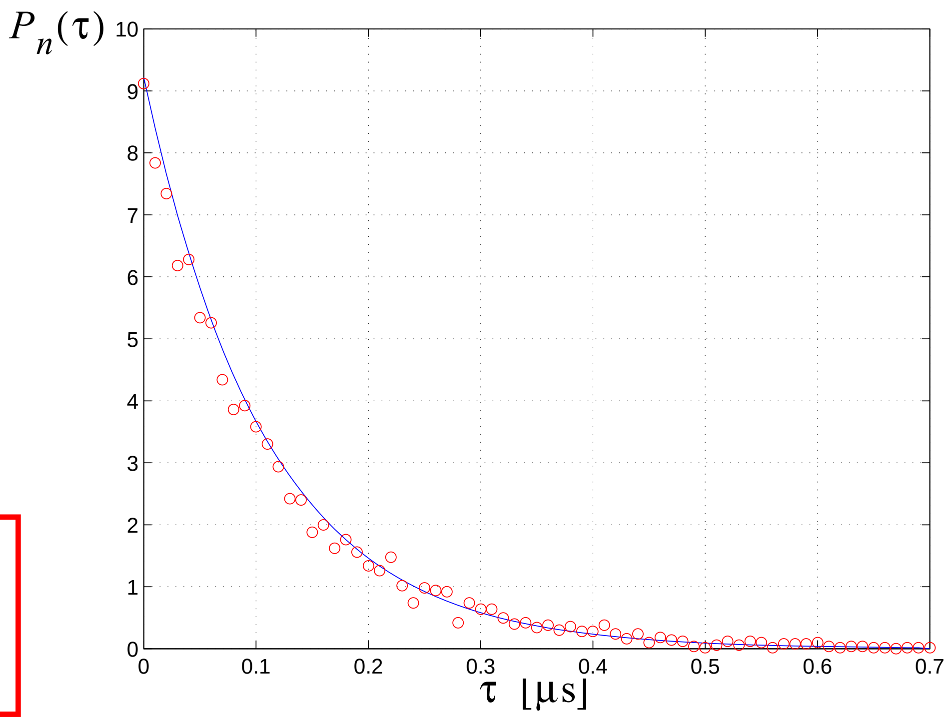

$$P_n(\tau) \propto \begin{cases} \exp(-9.2\tau) & ; \quad 0 \le \tau_{[\mu s]} \le 0.7 \\ 0 & ; \quad \text{elsewhere} \end{cases}$$

COST 207 model

Normalized delay scattering function (cont'd):

Typical hilly terrain (HT):

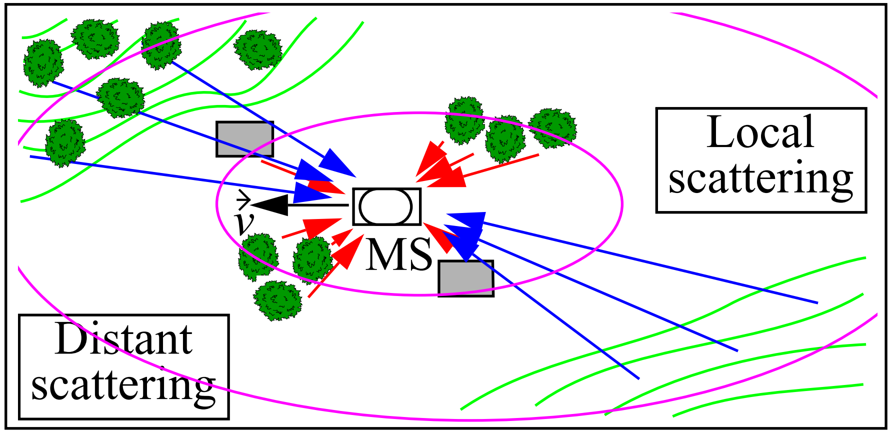

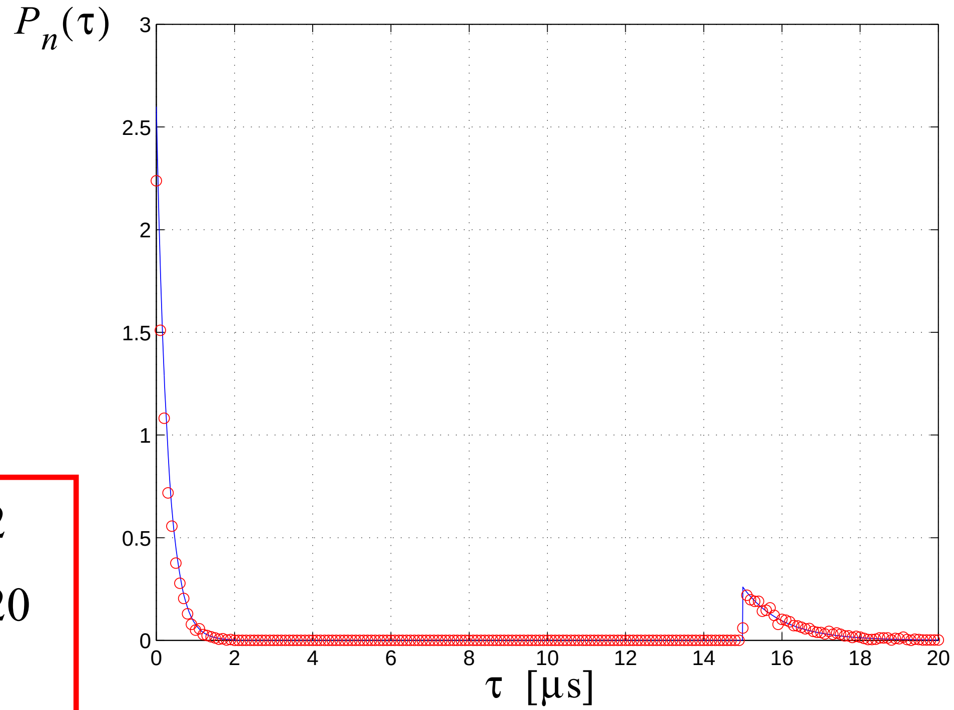

$$P_n(\tau) \propto \begin{cases} \exp(-3.5\tau) & ; \quad 0 \le \tau_{[\mu s]} \le 2 \\ 0.1\exp(15-\tau) & ; \quad 15 \le \tau_{[\mu s]} \le 20 \\ 0 & ; \quad \text{elsewhere} \end{cases}$$

COST 207 model

Normalized Doppler scattering function:

CLASS (Clarke's Doppler spectrum) $[\tau \leq 0.5\ \mu s]$:

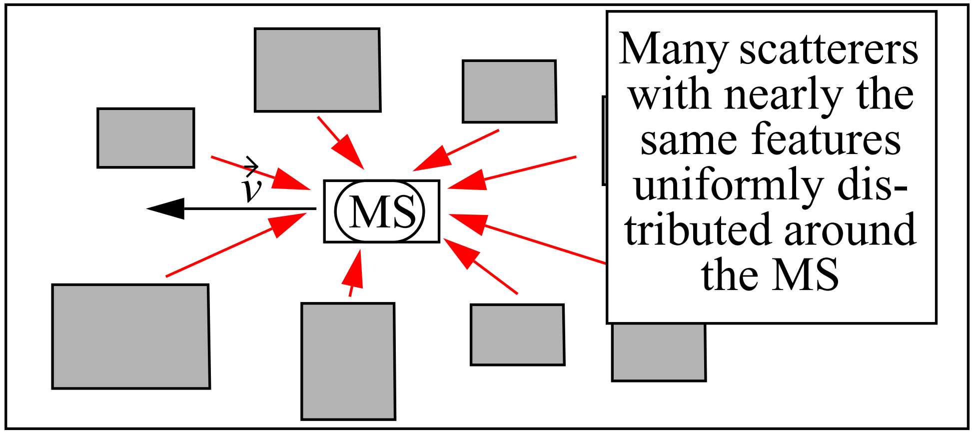

$$P_n(\nu|\tau) = \begin{cases} \dfrac{1}{\pi\nu_D} \dfrac{1}{\sqrt{1-(v/\nu_D)^2}} & ; \quad |\nu| < \nu_D \\ 0 & ; \quad \text{elsewhere} \end{cases}$$

$$\equiv C_{\nu_D}(\nu) \qquad (\nu_D \equiv v/\lambda)$$

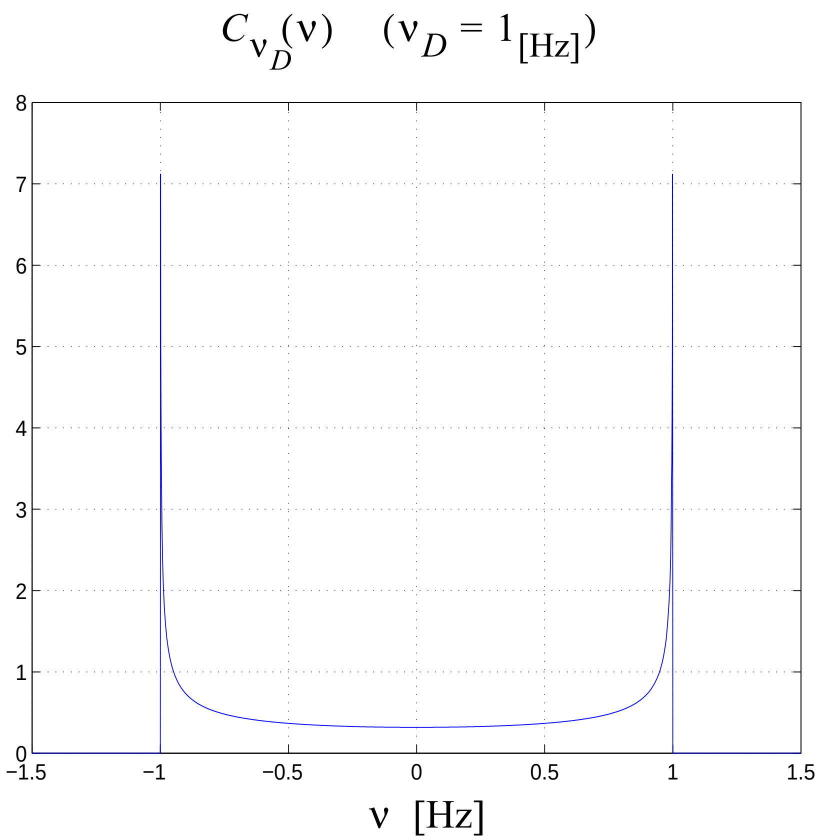

COST 207 model

Normalized Doppler scattering function (cont'd):

GAUS1 $[0.5\ \mu s \leq \tau \leq 2\ \mu s]$:

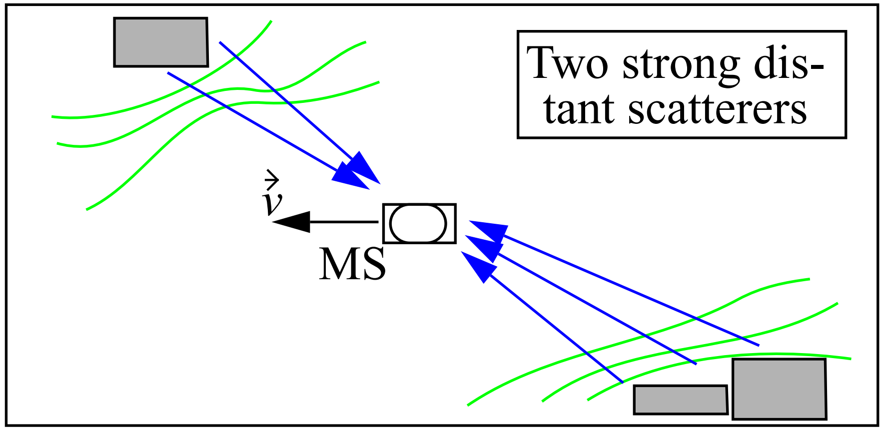

$$G(\nu; a, \nu_1, \nu_2) \equiv a \cdot \exp\left(-\frac{(\nu - \nu_1)^2}{2(\nu_2)^2}\right)$$

$$P_n(\nu|\tau) \propto G(\nu; a_1, -0.8\nu_D, 0.05\nu_D) + G(\nu; a_2, 0.4\nu_D, 0.1\nu_D)$$

with $\left(\frac{a_2}{a_1}\right)_{[\text{dB}]} = -10\ \text{dB}$

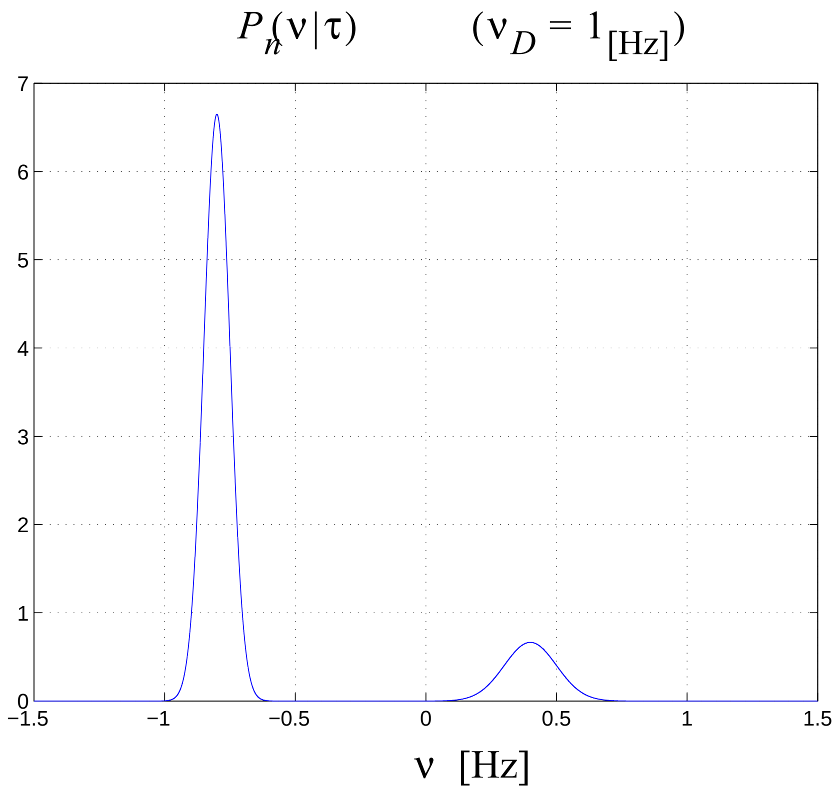

COST 207 model

Normalized Doppler scattering function (cont'd):

GAUS2 [μs $2 \leq \tau$]:

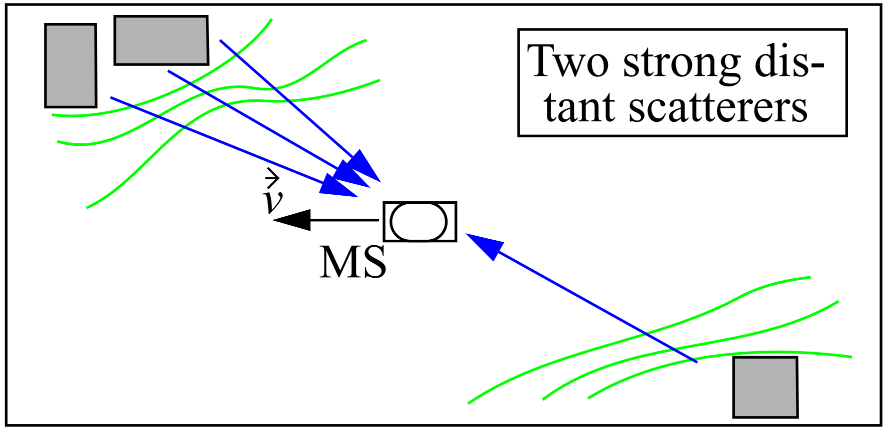

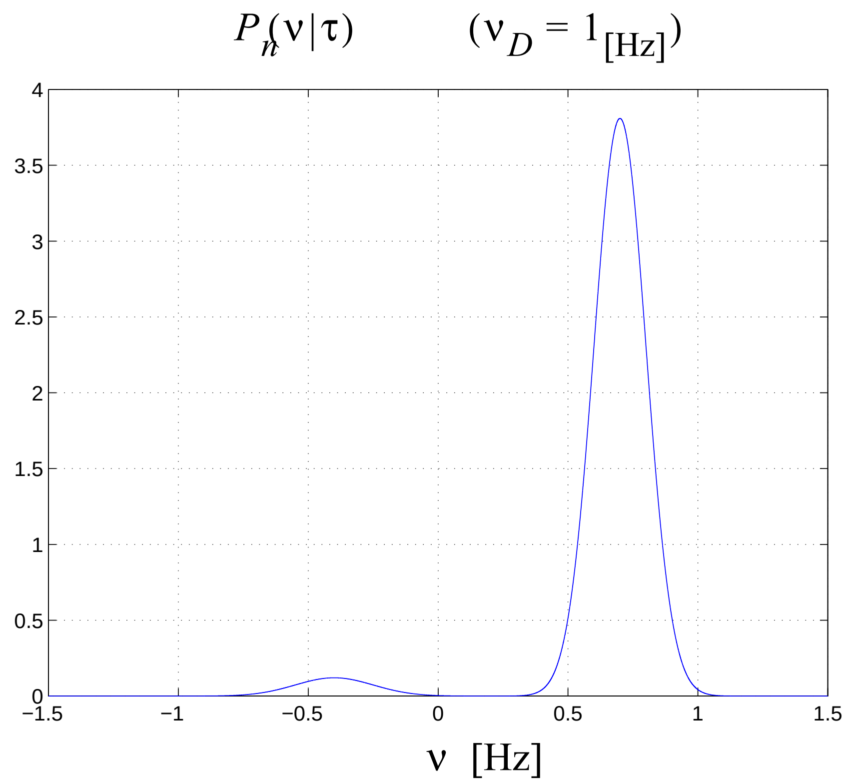

$$P_n(\nu|\tau) \propto G(\nu; a_1, 0.7\nu_D, 0.1\nu_D) + G(\nu; a_2, -0.4\nu_D, 0.15\nu_D)$$

$$\text{with } \left(\frac{a_2}{a_1}\right)_{[\mathrm{dB}]} = -15 \text{ dB}$$

COST 207 model

Normalized Doppler scattering function (cont'd):

RICE:

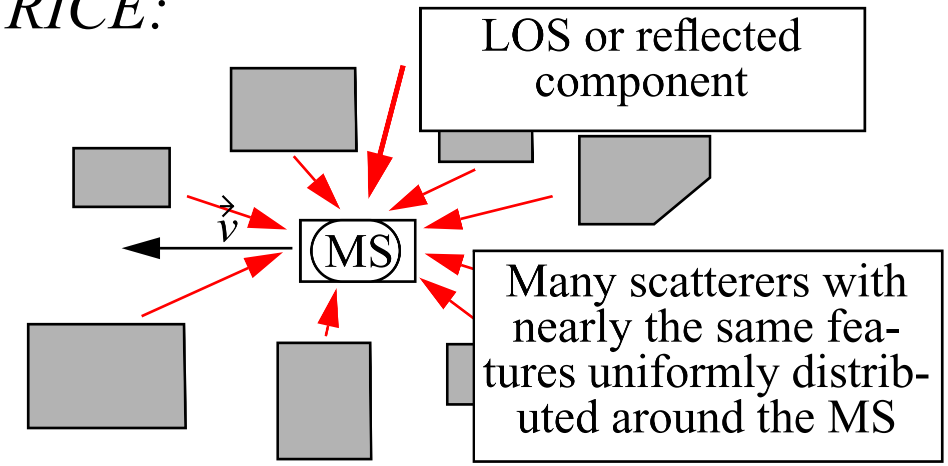

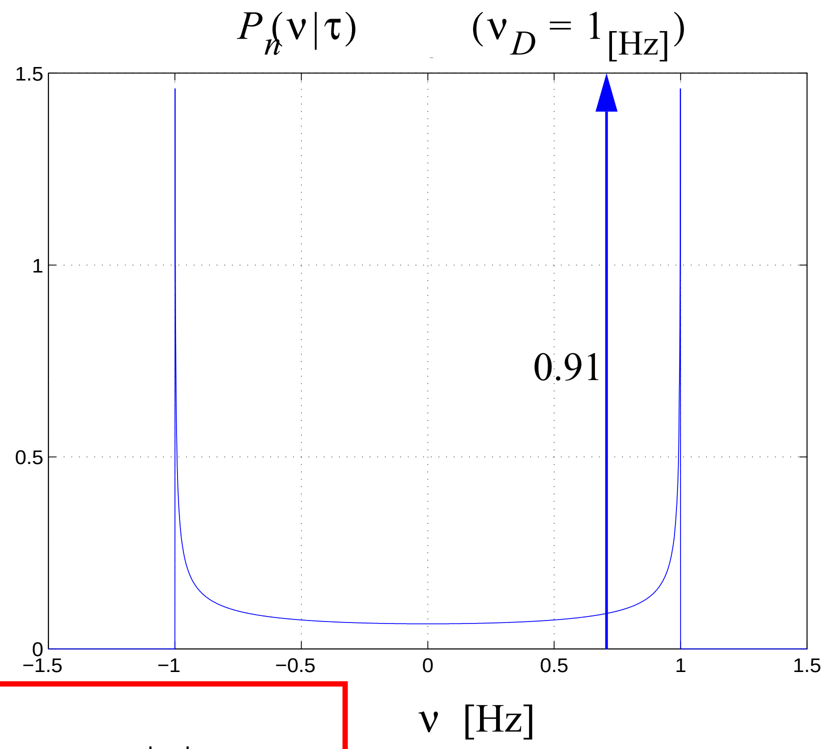

$$P_n(\nu|\tau) \propto \begin{cases} \dfrac{0.41}{2\pi\nu_D}\dfrac{1}{\sqrt{1-(\nu/\nu_D)^2}} + 0.91\delta(\nu - 0.7\nu_D) & ; \quad |\nu| < \nu_D \\ 0 & ; \quad \text{elsewhere} \end{cases}$$

COST 207 model

Simulation issues:

Make use of the following result:

If the random variables $\nu_1, \tau_1, \varphi_1, \nu_2, \tau_2, \varphi_2, \ldots, \nu_N, \tau_N, \varphi_N$ satisfy the following properties:

- the pairs (ν_i, τ_i) are independent with probability distribution $P_n(\nu, \tau)$,
- the phases φ_i are independent and uniformly distributed over $[0, 2\pi)$,
- the sequences $\{(\nu_i, \tau_i)\}$ and $\{\varphi_i\}$ are independent,

then for N sufficiently large, the scattering function of the simulated channel is close to $P(\nu, \tau)$.

COST 207 model

Simulated time-variant delay SF [TU]:

$$P_n(\nu|\tau) = C_{\nu_D}(\nu)$$

$\nu_D = 83.3$ Hz

(v=100 km/h, f= 900 MHz)

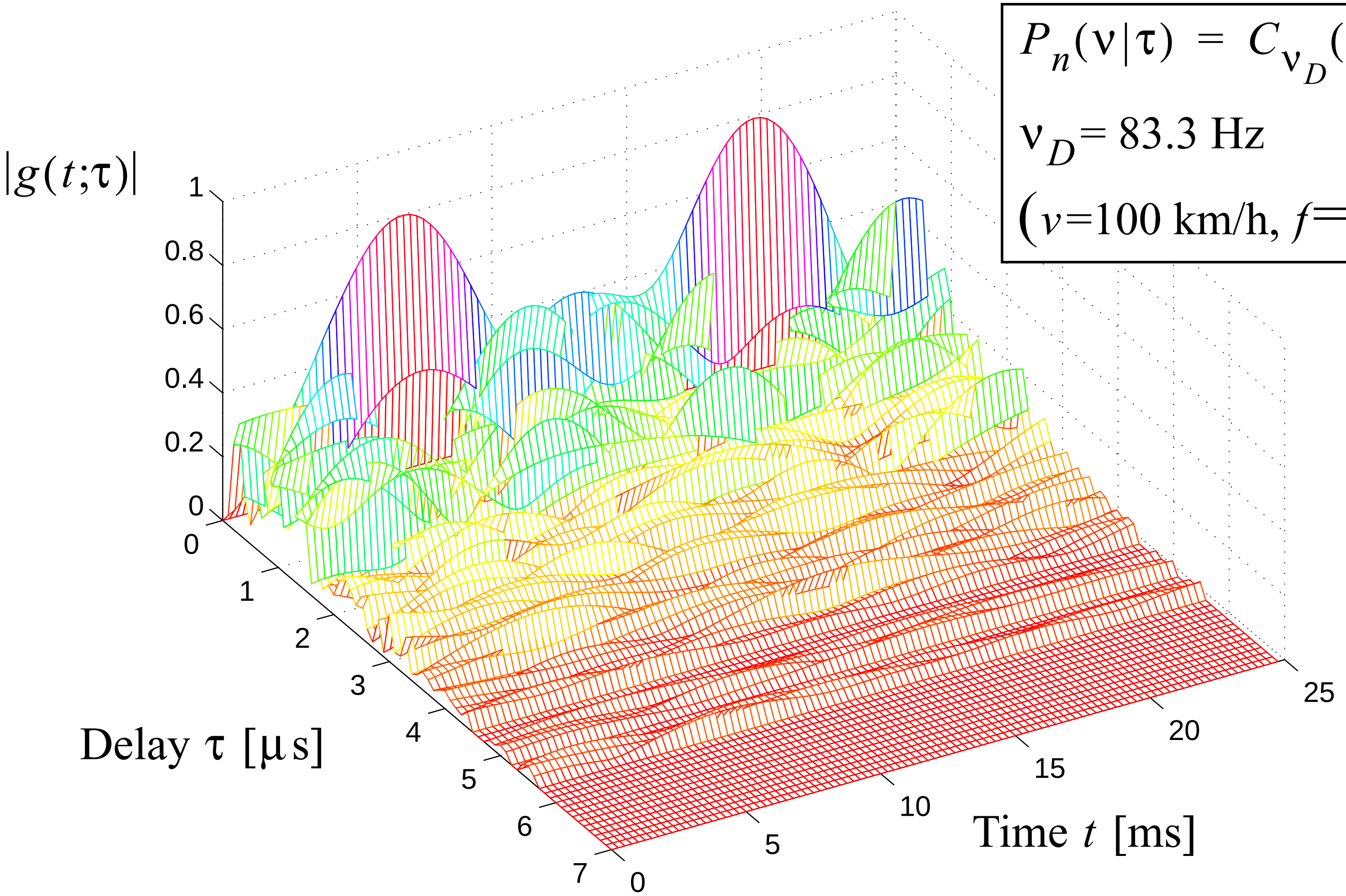

Source: ETHZ, CTL, R. Heddergott

COST 207 model

Simulated time-variant delay SF [BU]:

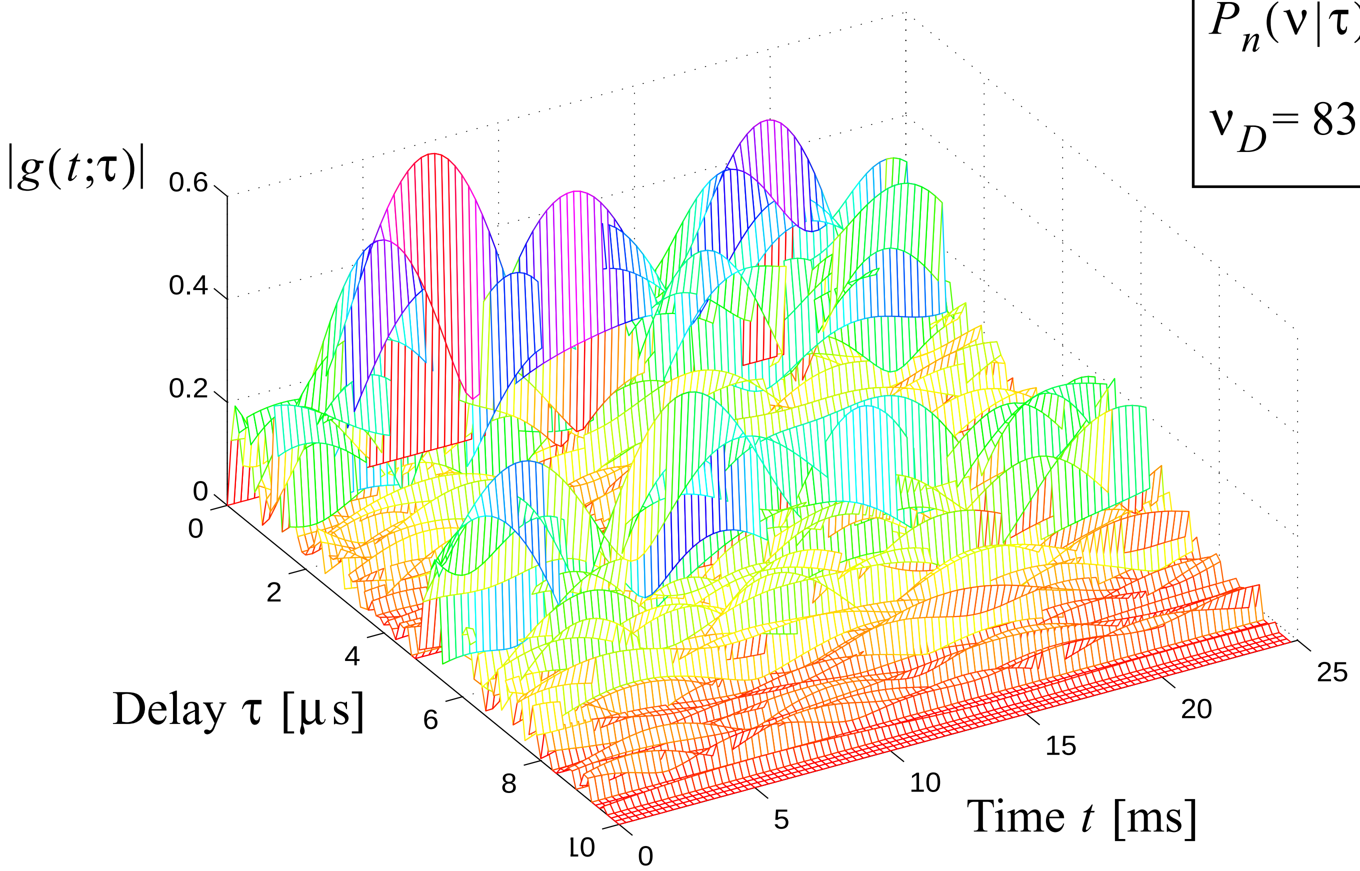

$P_n(\nu|\tau) = C_{\nu_D}(\nu)$

$\nu_D = 83.3$ Hz

Source: ETHZ, CTL, R. Heddergott

COST 207 model

Simulated time-variant delay SF [RA]:

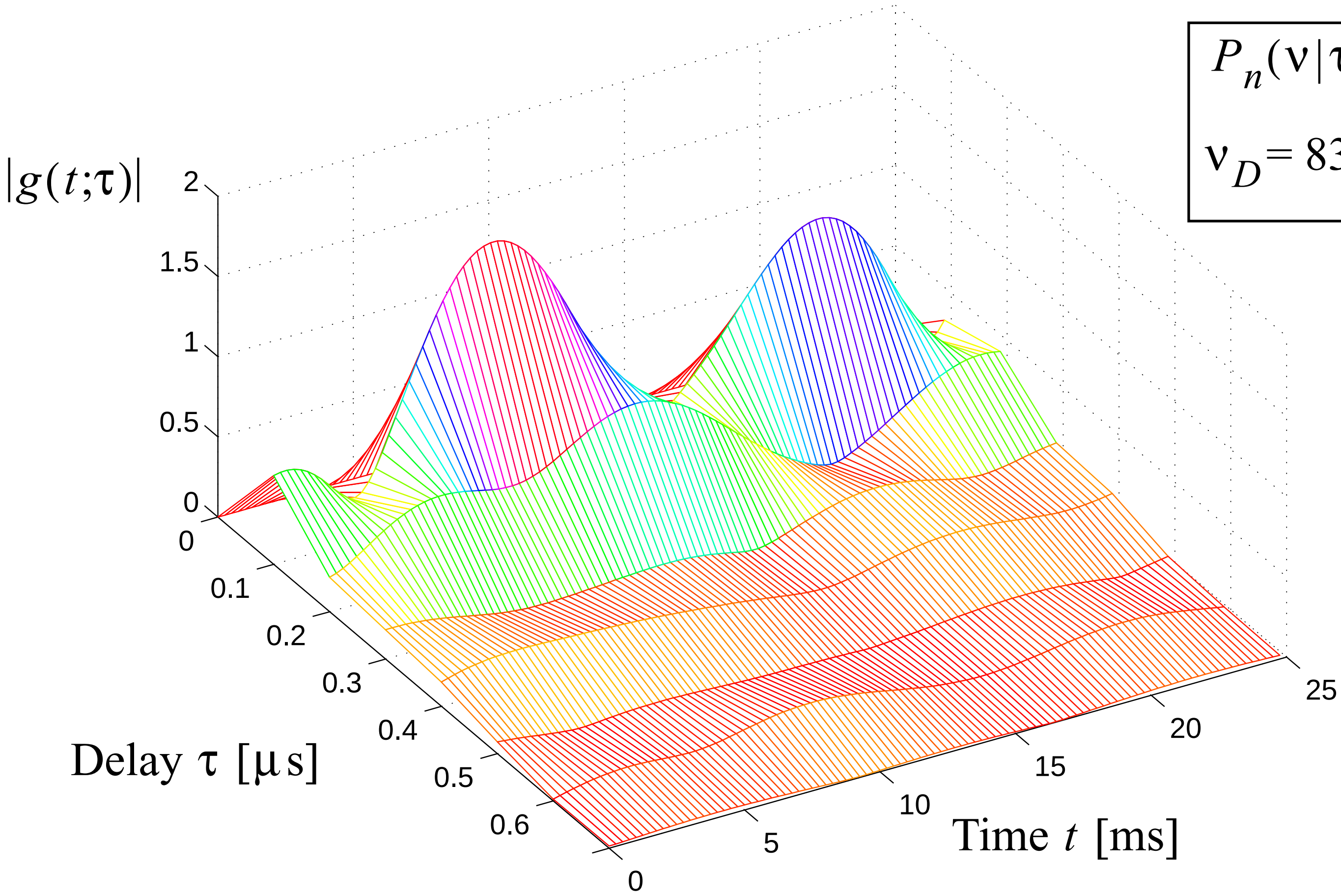

$$P_n(\nu|\tau) = C_{\nu_D}(\nu)$$

$\nu_D = 83.3$ Hz

Source: ETHZ, CTL, R. Heddergott

COST 207 model

Simulated time-variant delay SF [HT]:

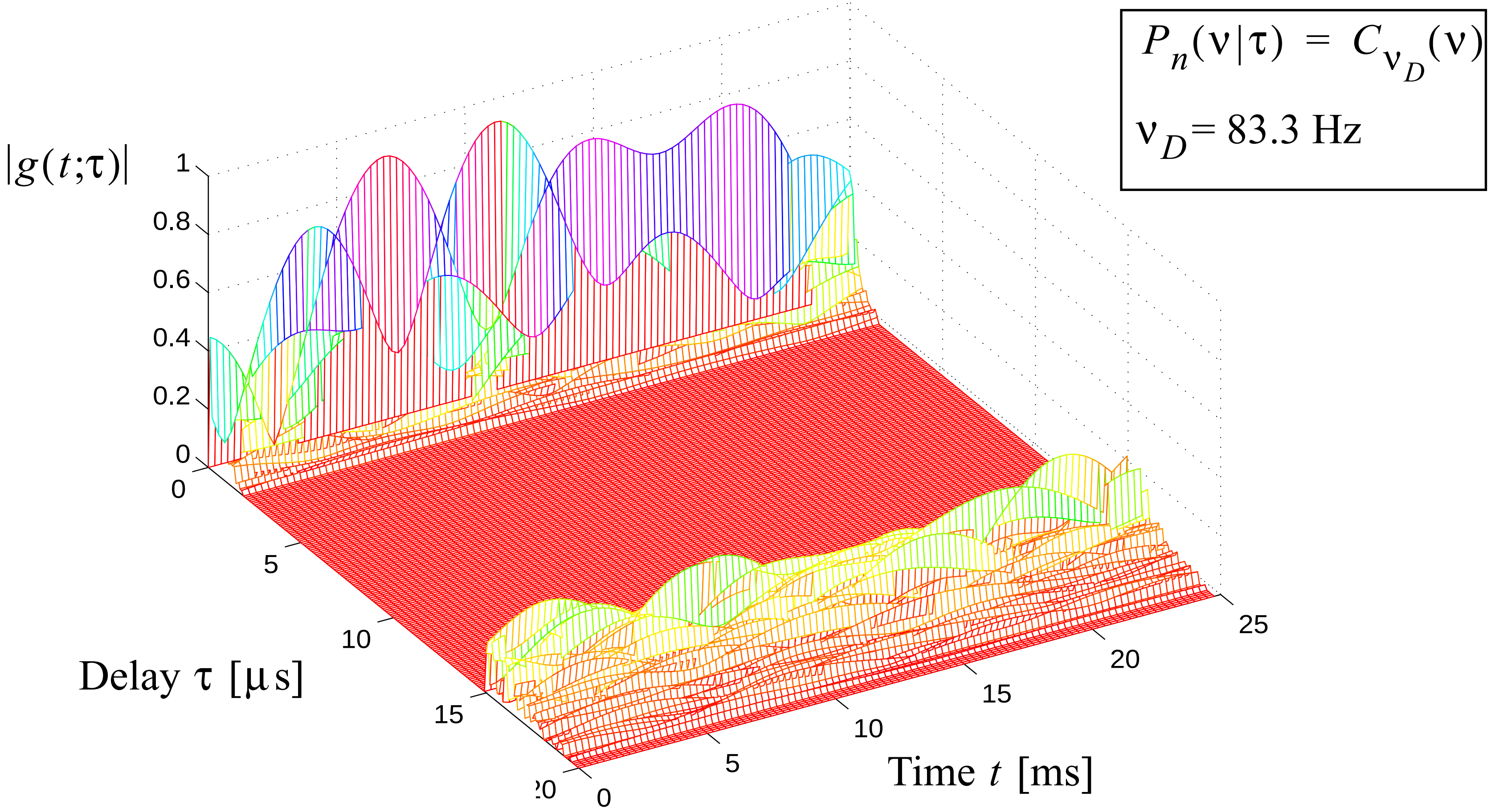

Source: ETHZ, CTL, R. Heddergott

COST 207 model

The COST 207 tables:

Example: BU

Tap No	Delay μ	Power [lin]	Power [dB]	Doppler spectrum
1	0.0	0.20	-7	CLASS
2	0.2	0.50	-3	CLASS
3	0.4	0.79	-1	CLASS
4	0.8	1.00	0	GAUS1
5	1.6	0.63	-2	GAUS1
6	2.2	0.25	-6	GAUS2

Tap No	Delay μ	Power [lin]	Power [dB]	Doppler spectrum
7	3.2	0.20	-7	GAUS2
8	5.0	0.79	-1	GAUS2
9	6.0	0.63	-2	GAUS2
10	7.2	0.20	-7	GAUS2
11	8.2	0.10	-10	GAUS2
12	10.0	0.03	-15	GAUS2

Delay spread: $\sigma_\tau = 2.5\ \mu s$

COST 207 model

The COST 207 tables (cont'd):

Delay scattering function for the BU model:

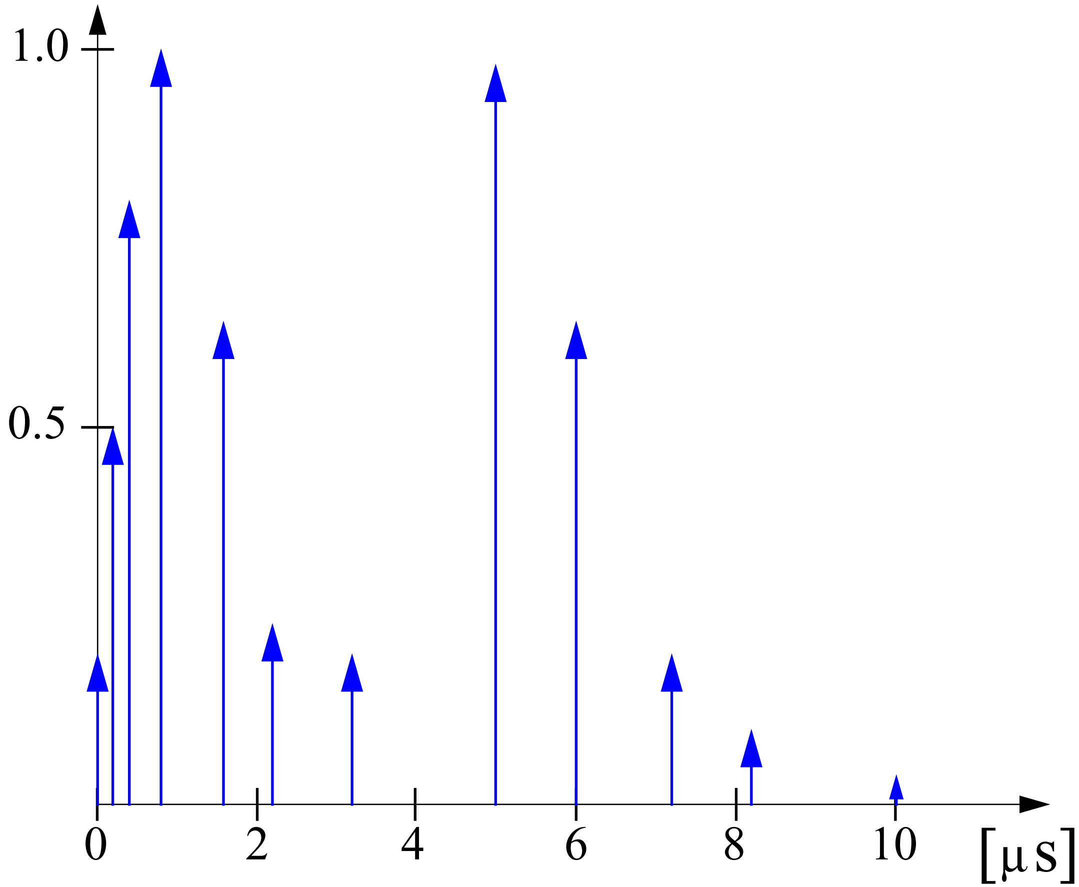

COST 207 model

The COST 207 tables (cont'd):

Comment:

!! The delays are regularly spaced !!

i.e., $\tau_i = m_i \Delta\tau$ with m_i integer and $\Delta\tau = 0.2\mu s$.

-> The transfer function is periodic (with period = 5 MHz)

-> The parameter settings in the COST 231 tables are not appropriate for investigating the performance of systems which exploit channel frequency selectivity,
e.g. GSM with frequency hopping.

Solution:

Choose an irregularly spacing of the delays or randomly select them.

COST 207 model

The COST 207 tables (cont'd):

Frequency hopping:

Real channel frequency transfer function:

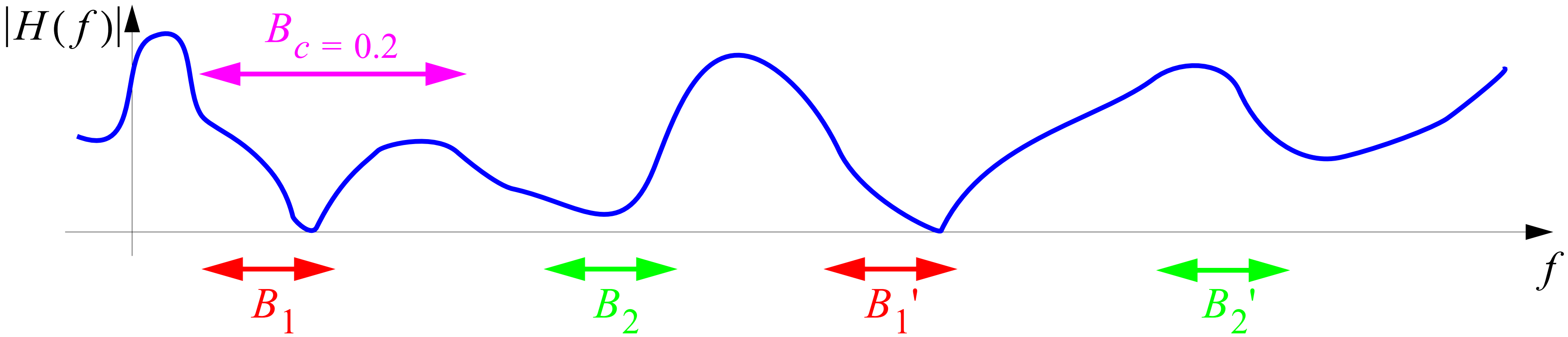

Transfer function of the COST 207 channel:

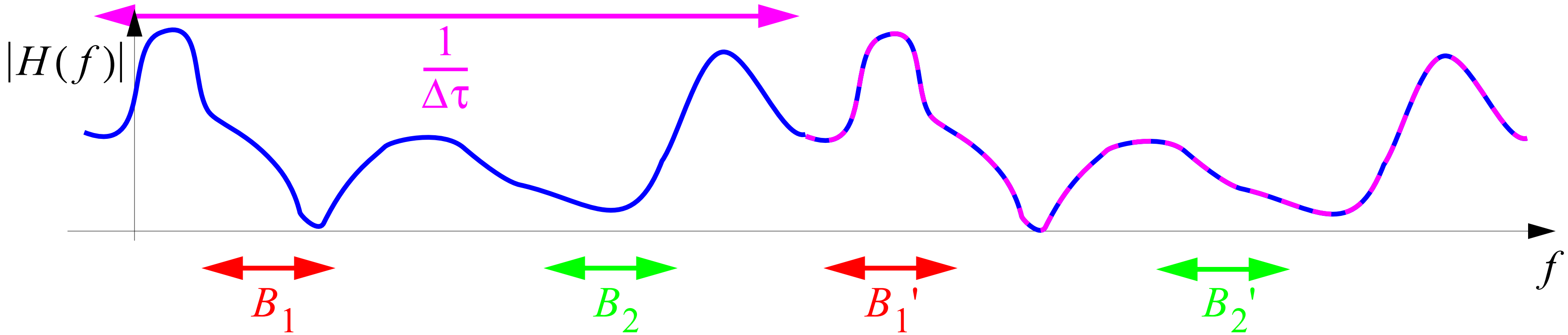

CODIT model

Main characteristics:

Cell type	• Macro-, micro, picocell
Area	• Macrocell: urban, suburban, suburban hilly rural, rural hilly • Microcell: dense urban linear street, town square, industrial area • Indoor: floor cell in buildings, corridor, large and very large rooms
Frequency band	• 2 GHz range • Up to 20 MHz signal bandwidth
Time-variant SF	• $g(t;\tau) \equiv \sum_{i=1}^{N} g_i(t) \cdot \delta(\tau - \tau_i(t))$
Input	• Area type • Vehicle velocity • System bandwidth

CODIT model

Short-term variations of $g_i(t)$:

$$\boxed{g_i^{(\mathrm{ST})}(t) = \underbrace{h_{i,c}\exp\left(j2\pi\overbrace{\frac{v}{\lambda}\cos(\phi_{i,c})}^{\nu_{i,c}}t\right)}_{\text{Specular part}} + \underbrace{\sum_{j=1}^{J} h_{i,j}\exp\left(j2\pi\overbrace{\frac{v}{\lambda}\cos(\phi_{i,j})}^{\nu_{i,j}}t\right)}_{\text{Diffuse part}}}$$

- $|h_{i,c}| = \sigma_{i,c}$,
- $\arg\{h_{i,c}\}$ uniformly distributed over $[0, 2\pi)$
- $h_{i,j} \sim \mathcal{N}\left(0, \frac{1}{J}\sigma_{i,d}^2\right)$
- $\mathbf{E}[|g_i(t)|^2] = \sigma_{i,c}^2 + \sigma_{i,d}^2 \equiv \sigma_i^2$: mean power of the ith component
- $(\sigma_{i,c}/\sigma_{i,d})^2$: coherent to diffuse power ratio of the ith component

CODIT model

Probability distribution of the azimuths $\phi_{i,c}$ and $\phi_{i,j}$:

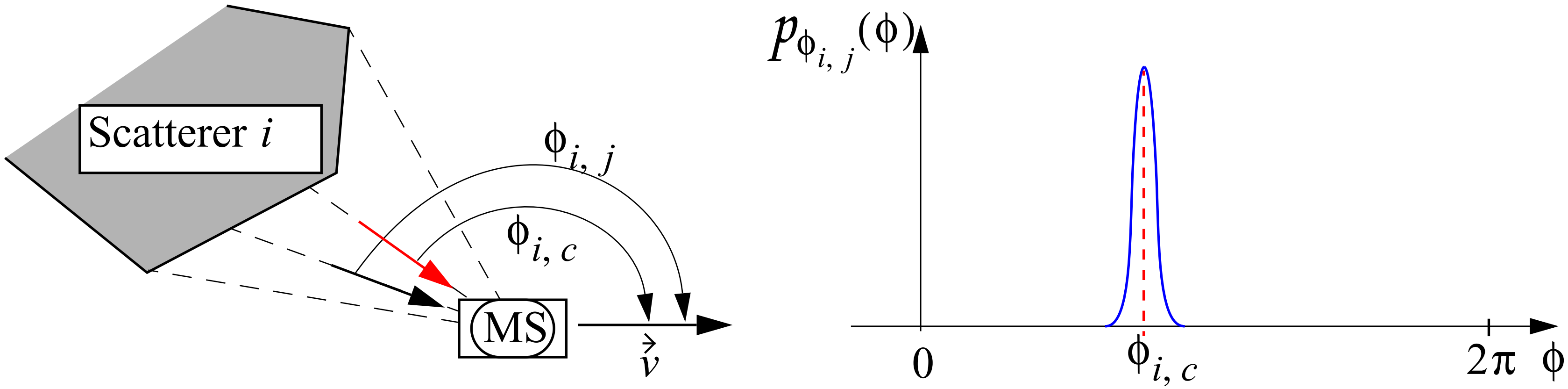

$$\phi_{i,j} \sim \mathcal{N}(\phi_{i,c}, 0.15^2_{[\text{radian}]})\Big|_{\text{mod}2\pi}$$

CODIT model

Long-term variations of $g_i(t)$:

$$\boxed{g_i(t) \;=\; z_i(t)\cdot g_i^{(\mathrm{ST})}(t)}$$

Term describing the long-term fluctuations

Shadowing effects:

$$\boxed{z_i(t) \equiv 1 + \Delta z_i \cdot \cos\left(\frac{2\pi}{q_i}\frac{v}{\lambda}t + \psi_i\right)}$$

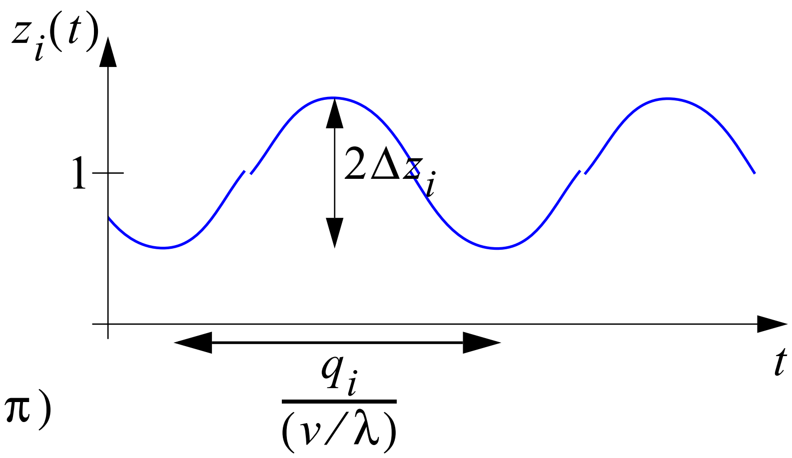

ψ_i: Random variable uniformly distributed over $[0, 2\pi)$

CODIT model

Long-term variations of $g_i(t)$ (cont'd):

Emergence of the components:

$$\boxed{z_i(t) \equiv \begin{cases} \dfrac{1}{1+\left(\dfrac{vt-z}{5\lambda}\right)^6} & ; \quad vt \le z \\ 1 & ; \quad vt > z \end{cases}}$$

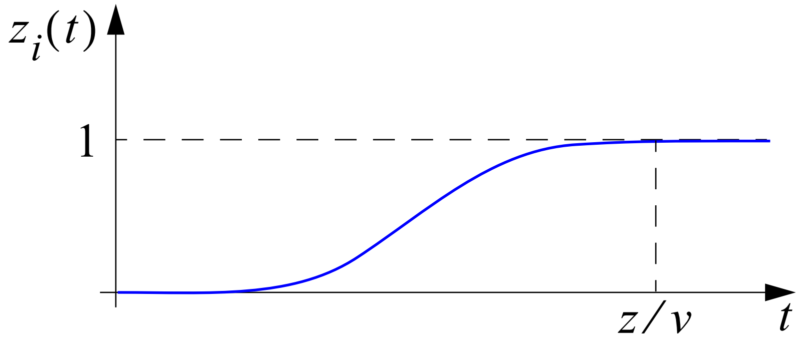

Fading of the components:

$$\boxed{z_i(t) \equiv \begin{cases} \dfrac{1}{1+\left(\dfrac{vt-z}{5\lambda}\right)^6} & ; \quad vt \ge z \\ 1 & ; \quad vt < z \end{cases}}$$

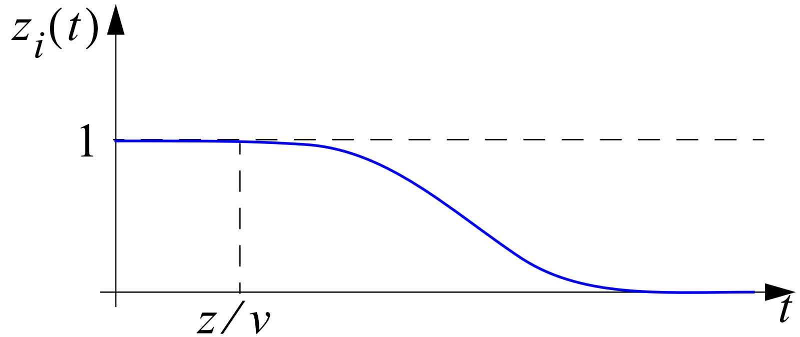

z is a random variable uniformly distributed over $[50\lambda, 70\lambda]$.

CODIT model

Short-term variations of $\tau_i(t)$ **:**

$$\boxed{\tau_i(t) = \tau_i}$$

Long-term variations of $\tau_i(t)$ **:**

$$\boxed{\tau_i(t) = \tau_i + \Delta\tau_i\left[1 + \cos\left(\frac{2\pi}{p_i}\frac{v}{\lambda}t + \upsilon_i\right)\right]}$$

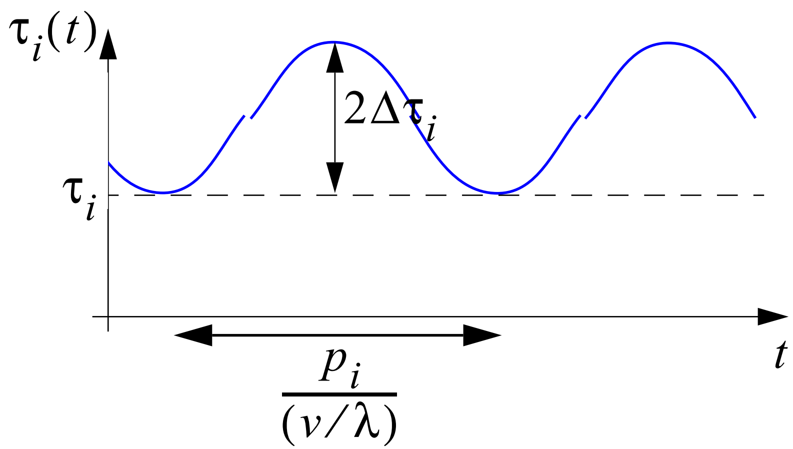

υ_i: Random variable uniformly distributed over $[0, 2\pi)$

CODIT model

Selection of the parameters of $g(t;\tau)$:

- The number N of components depends on the area type but is fixed for a given area, $N_{\max} = 20$.
- $J = 100$
- The parameters σ_i^2, $(\sigma_{i,c}/\sigma_{i,d})^2$, $\phi_{i,c}$, Δz_i, q_i, τ_i, $\Delta\tau_i$, p_i describing the behaviour of the components of $g_i(t)$ are random variables specified by probability distributions.

CODIT model

Setting Tables:

Example: Suburban hilly environment**:**

Summary of values for suburban hilly environment:

Nr. scatterers N=20							
Scatterer	σ_i^2	$\frac{\mathbf{E}[\lvert h_i\rvert^2]^2}{\mathbf{Var}[\lvert h_i\rvert^2]}$	ϕ_i	$\tau_i\ [\mu s]$	Δz_i	$q_i \quad p_i$	$\Delta\tau_i\ [ns]$
1	1	15	[0,π]	0	[0,0.7]	[1000,2000]	0
2-6	[0.1,0.4]	[1,5]	[0,π]	[0.1,15]	[0.1,1]	[500,1000]	[0,400]
Cluster: 7-20	[0,0.1]	1	(a)	(b)	0	Not Applicable	0

(a) The arriving angles will be approximately the same for all the scatterers in the cluster.
(b) Sorted within a delay window of 10 µs in the range 15-80 µs.

$$\sum_i^N \sigma_i^2 = 1$$

Source: CODIT Report: Final Propagation Model

CODIT model

Setting Tables (cont'd):

Example: Power delay spectrum generated with the previous table:

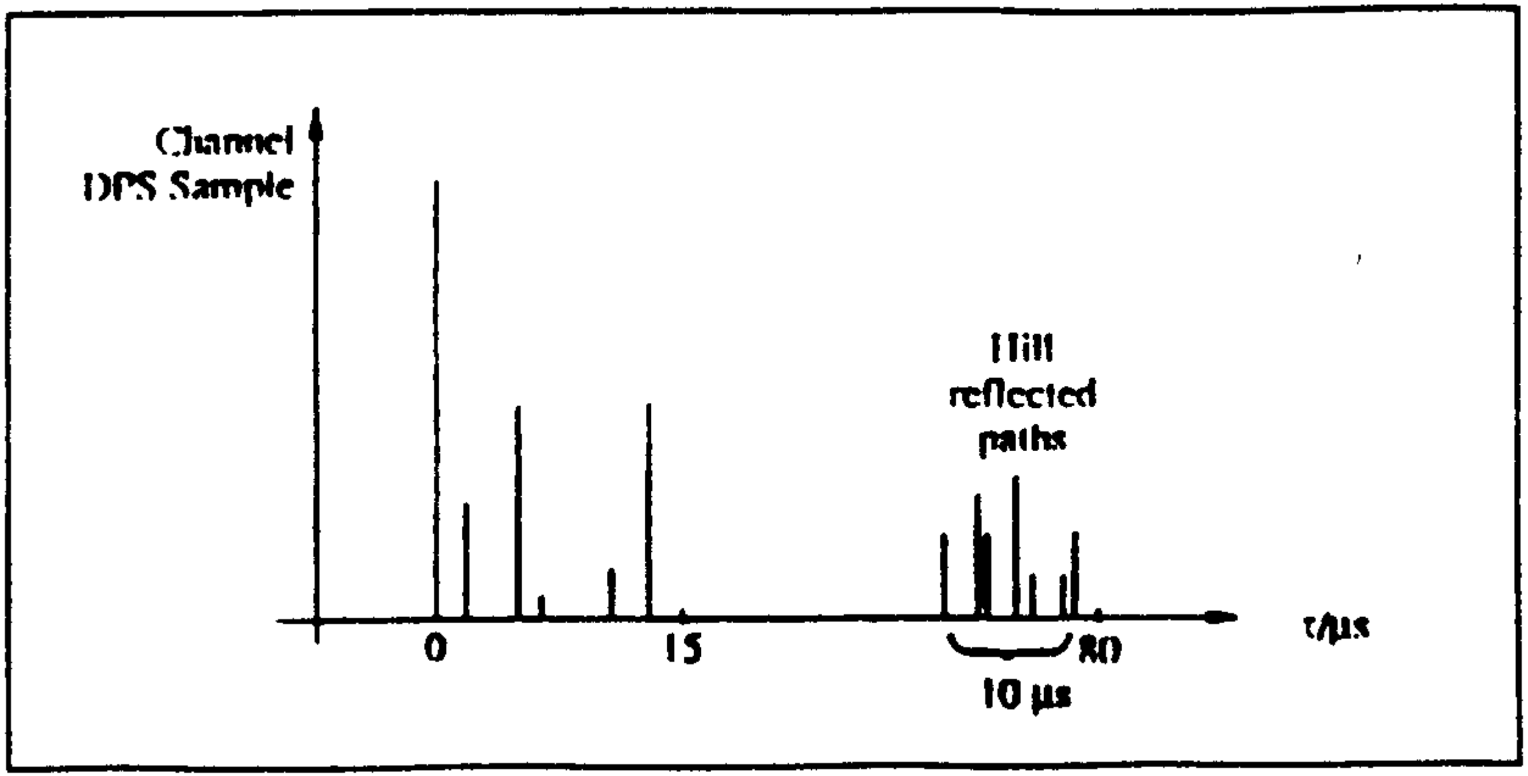

Figure 3.13 Sample of a suburban hilly delay power spectrum

Source: CODIT Report: Final Propagation Model

CODIT model

Example: “Microcell LOS Area”:

Contour plot of a realization of $|g(d;\tau)|$:

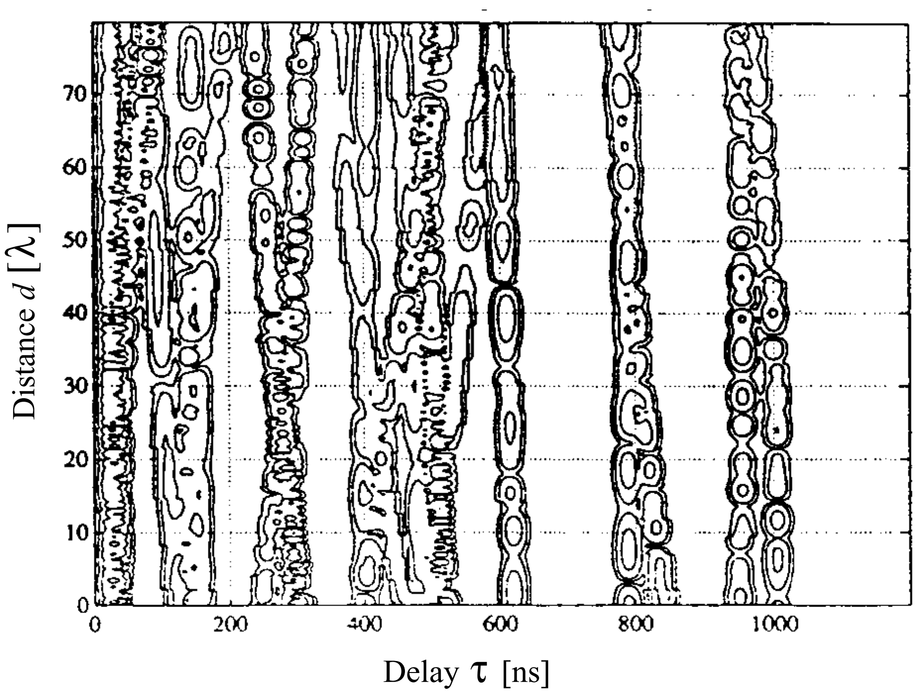

Evolution of the corresponding delay scattering function

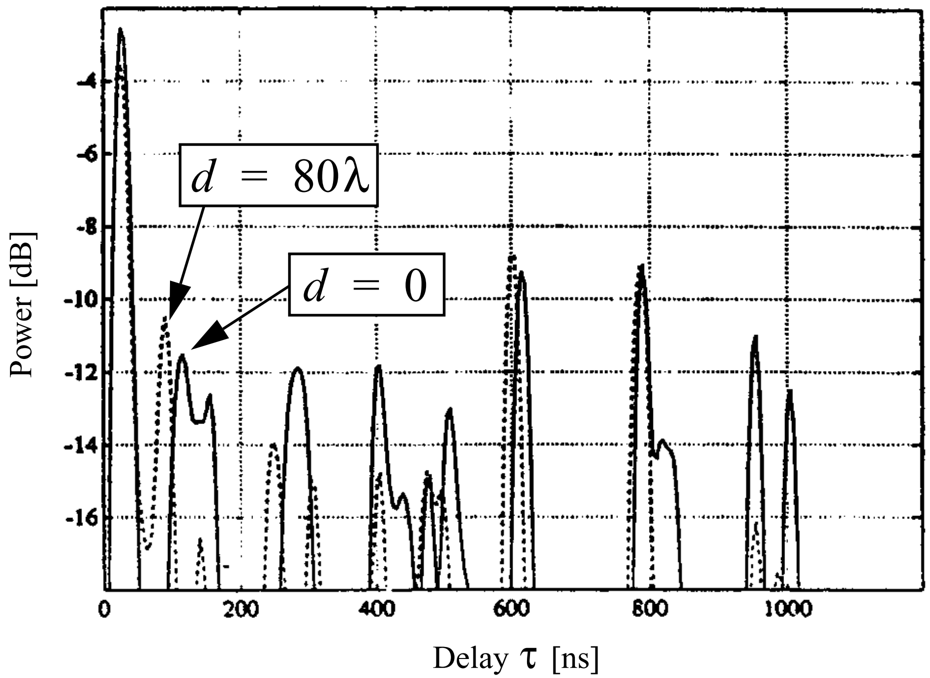

Source: CODIT Report: Final Propagation Model

CODIT model

Example: “Indoor Picocell LOS Area”:

Contour plot of a realization of $|g(d;\tau)|$:

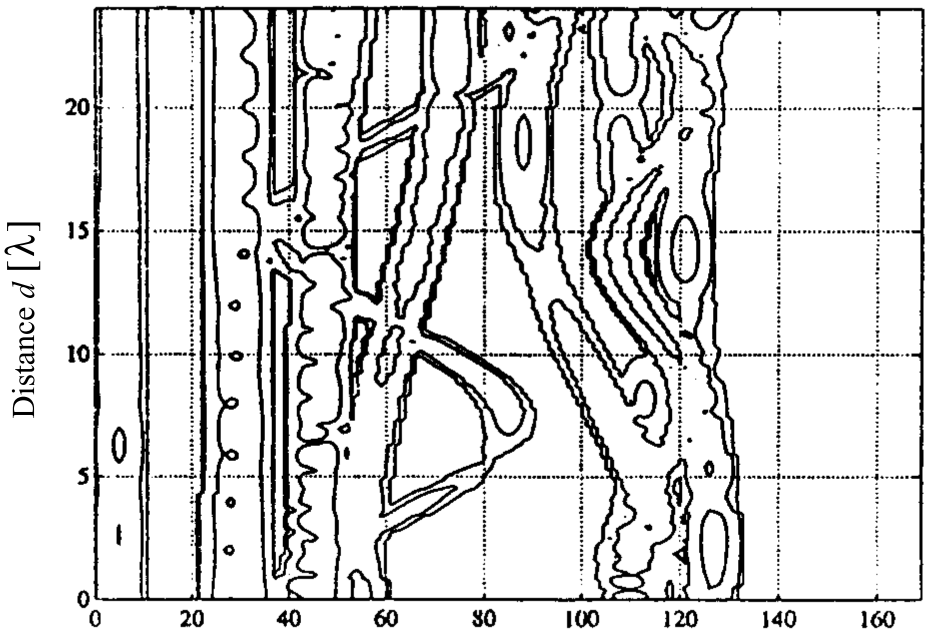

Evolution of the corresponding delay scattering function

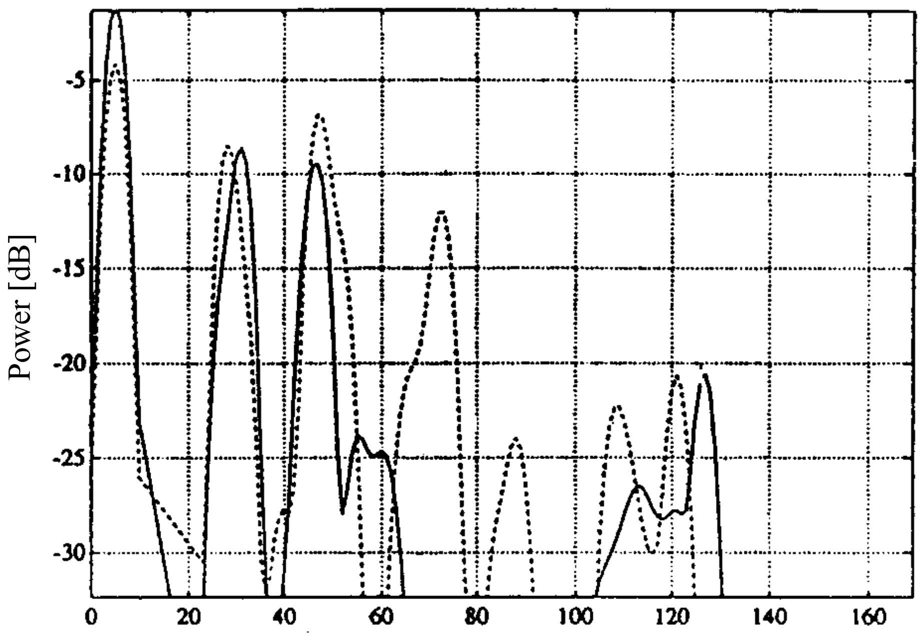

Source: CODIT Report: Final Propagation Model

Turin-Suzuki-Hashemi model

Main characteristics:

Cell type	• Macro-, micro- and picocell (by appropriately setting the probability densities of model parameters)
Area	• Urban
Frequency range	• 500MHz -1GHz
Time-invariant delay SF	• $g(t;\tau) = h(\tau) = \sum_{i=1}^{N} h_i \cdot \delta(\tau - \tau_i)$
Main features	• Time-invariant • Clustering of the components in $h(\tau)$ is reproduced by modelling the sequence $\{\tau_i\}$ as a Poisson point process or a modification thereof.

Turin-Suzuki-Hashemi model

Modelling $\{\tau_i\}$ as a Poisson point process:

$\{\tau_i\}$ is a Poisson point process with rate $\gamma(\tau)$:

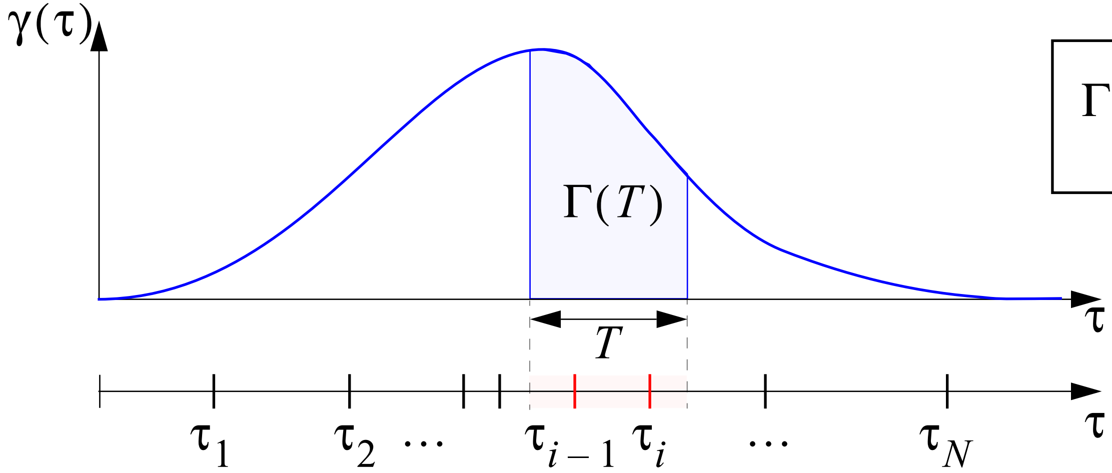

$$\Gamma(T) \equiv \int_T \gamma(\tau)\, d\tau$$

N_T: Number of points in the time interval T

$$\boxed{\mathbf{P}[N_T = n] = \frac{\Gamma(T)^n}{n!} \exp(-\Gamma(T))} \qquad [\ \mathbf{E}[N_T] = \mathbf{Var}[N_T] = \Gamma(T)]$$

Turin-Suzuki-Hashemi model

Modelling $\{\tau_i\}$ as a homogeneous Poisson point process:

$$\boxed{\gamma(\tau) = \gamma}$$

In this case, the delay differences $\tau_i - \tau_{i-1}$ are independent random variables which are (identically) exponentially distributed with parameter γ:

Probability density of $\tau_i - \tau_{i-1}$:

$$\boxed{p_{\tau_i - \tau_{i-1}}(\tau) = \gamma \exp(-\gamma\tau)}$$

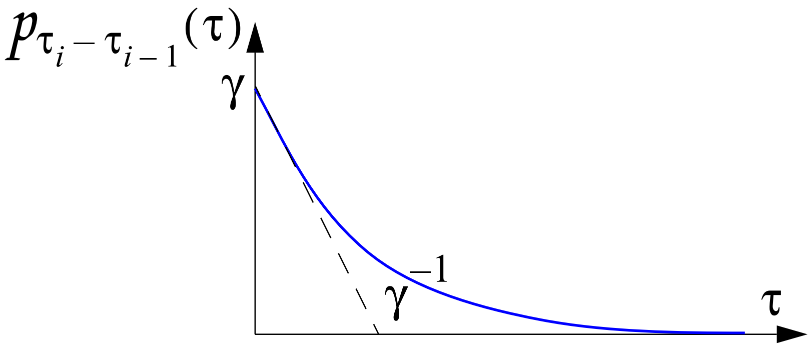

Drawback of the Poisson model:

It does not describe sufficiently accurately the clustering of the components as observed in measured delay SFs.

Turin-Suzuki-Hashemi model

Estimated rates in outdoor environments:

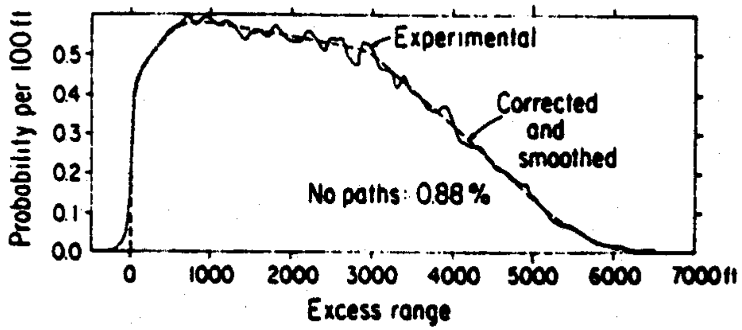

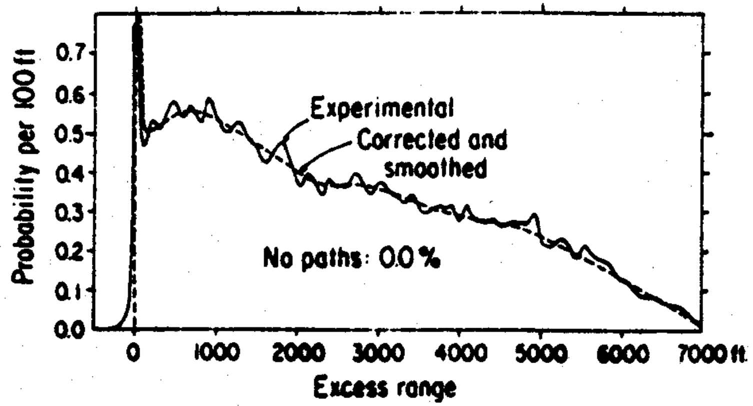

$1\,\mathrm{ft} \equiv 1\,\mathrm{ns}$

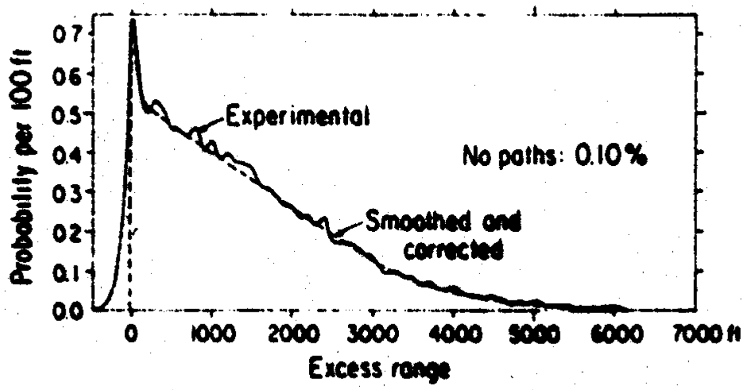

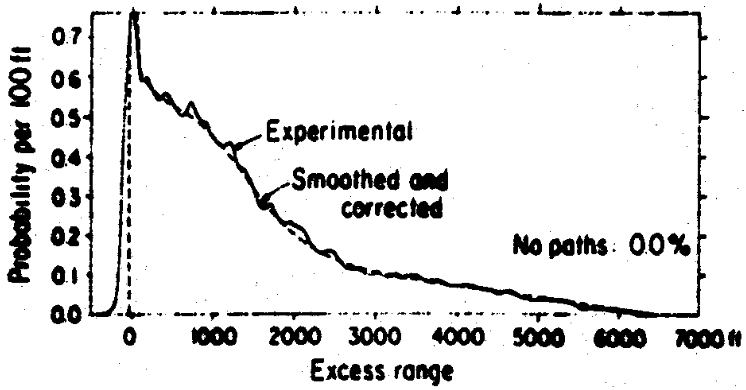

Source: Paper by Turin at al.

Turin-Suzuki-Hashemi model

Modelling $\{\tau_i\}$ as a modified Poisson point process:

The rate $\gamma(\tau)$ depends on the random sequence $\{\tau_i\}$ in the following way:

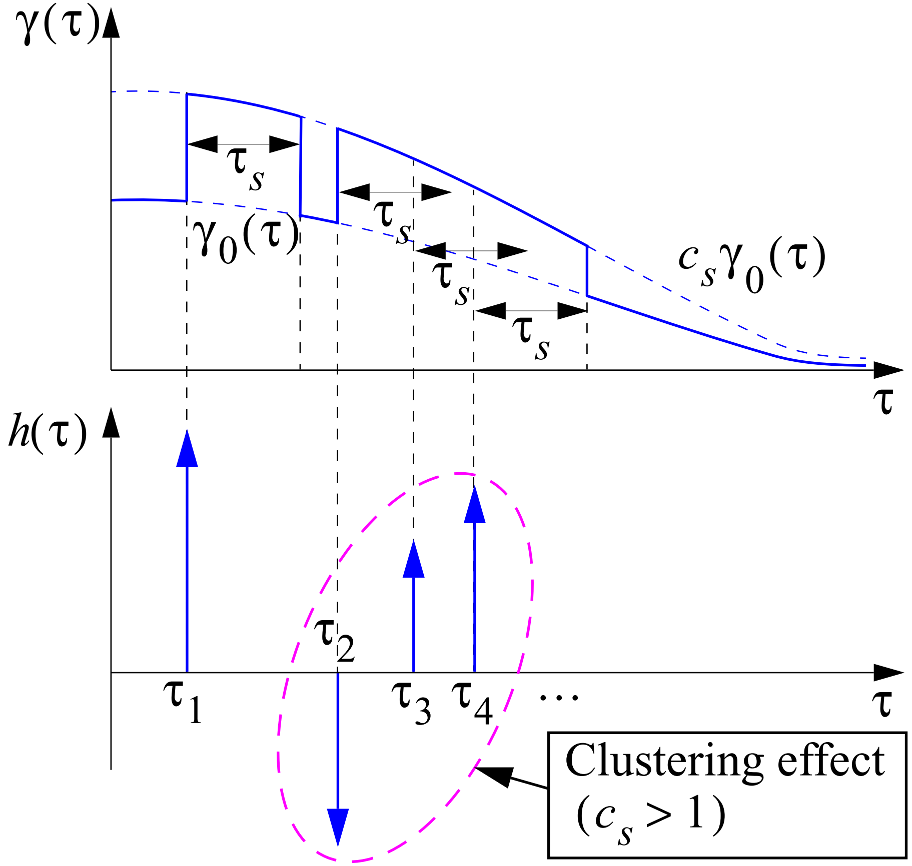

The basic rate $\gamma_0(\tau)$ is multiplied by a factor c_s during a predetermined relaxation interval τ_s at each τ_i:

- $c_s > 1$: Clustering effect
- $c_s = 1$: Poisson point process
- $c_s < 1$: Isolated delay points

Values for τ_s and τ_i (macrocell):

- $\tau_s = 100$ ns (arbitrarily selected)
- $0.1 < c_s < 3$ (estimated from measurements)

Turin-Suzuki-Hashemi model

Probability distribution of the coefficients h_i:

- The distribution of the amplitude $|h_i|$ is log-normal, i.e. $20\log(|h_i|)$ is a Gaussian random variable with a mean μ_h and a standard deviation σ_h. Both quantities depend on τ_i.
- The phase $\arg\{h_i\}$ is uniformly distributed over $[0, 2\pi)$.

Turin-Suzuki-Hashemi model

Probability distribution of the coefficients h_i (cont'd):

Two examples showing the behaviour of $\mu_h(\tau)$ and $\sigma_h(\tau)$ for macrocells:

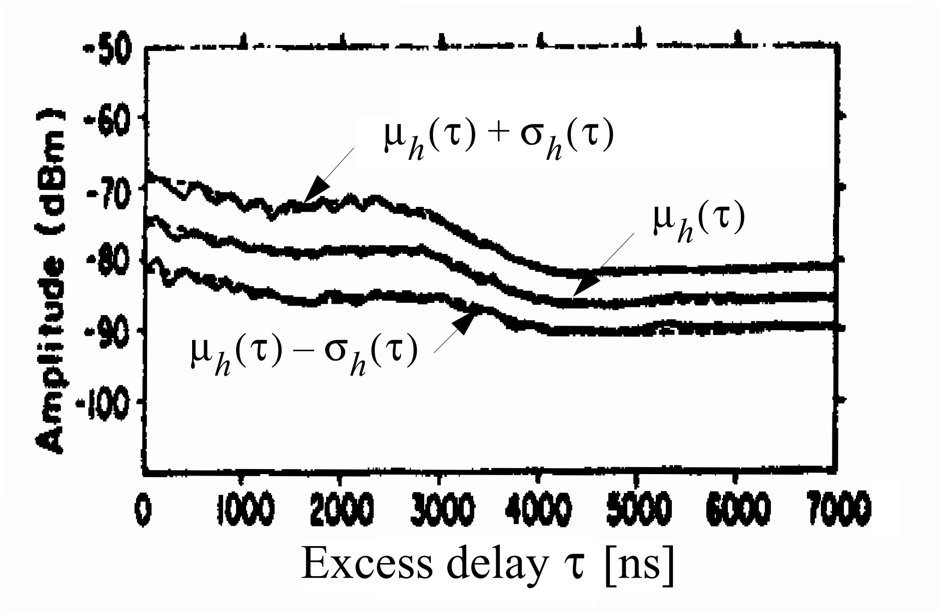

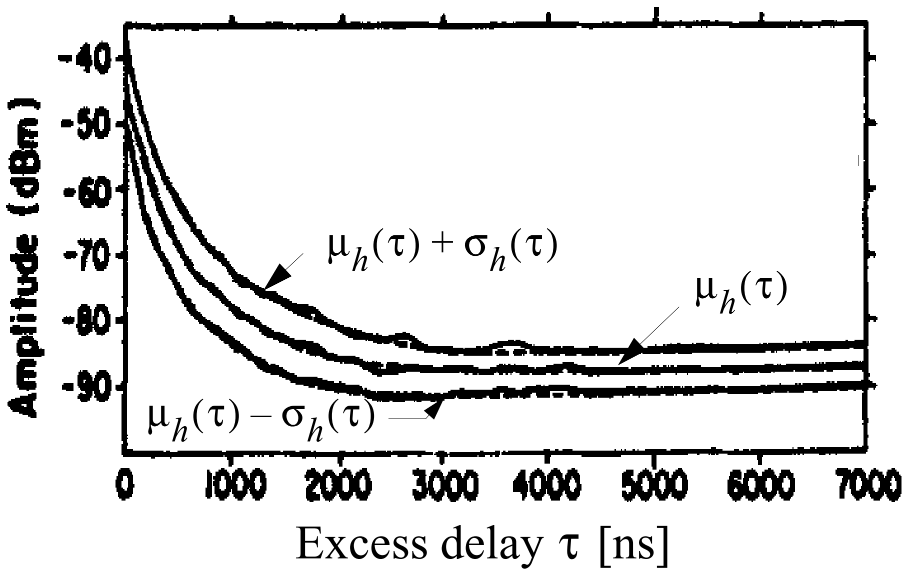

Source: Paper by Turin at al.

Saleh-Valenzuela model

Main characteristics:b

Cell type	• Picocell
Area	• Indoor
Frequency range	• Around 1GHz
Time-invariant delay SF	• $g(t;\tau) = h(\tau) = \sum_{i=0}^{N} \sum_{j=0}^{J(i)} h_{i,j} \cdot \delta(\tau - \tau_{i,j})$ i: Cluster index j: Index for the components within the clusters
Main features	• Static model • The clustering of the components in $h(\tau)$ is reproduced by modelling the sequence $\{\tau_{i,j}\}$ as a concatenation of two Poisson point processes

Saleh-Valenzuela model

Modelling $\{\tau_{i,j}\}$ as a concatenation of two Poisson point processes:

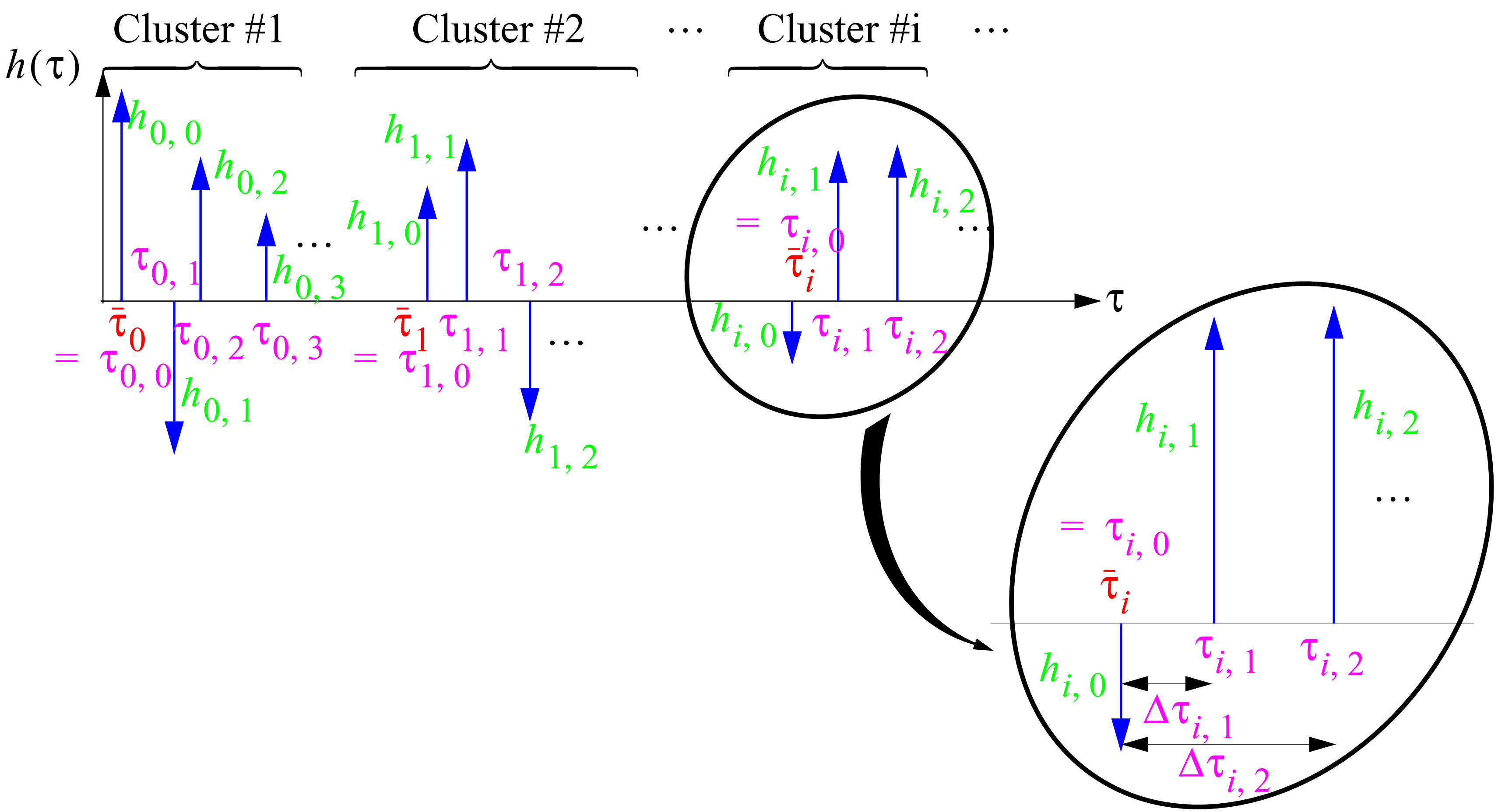

Saleh-Valenzuela model

Modelling $\{\tau_{i,j}\}$ as a concatenation of two Poisson point processes:

- Cluster delays $\{\bar{\tau}_i\}$: (i) $\bar{\tau}_0 = 0$

  (ii) $\{\bar{\tau}_i; i = 1, 2, \ldots, N\}$: Poisson process with rate Λ.

- Delays within cluster i:

  (i) $\tau_{i,0} = \bar{\tau}_i, \ldots, \tau_{i,j} \equiv \bar{\tau}_i + \Delta\tau_{i,j}$; $j = 1, 2, \ldots, J(i)$

  (ii) $\{\Delta\tau_{i,1}, \Delta\tau_{i,2}, \ldots\}$: Poisson process with rate λ.

Experimentally obtained values for Λ and λ:

- $1/\Lambda = 200 - 300$ ns
- $1/\lambda = 5 - 10$ ns

Saleh-Valenzuela model

Probability distribution of the coefficients $h_{i,j}$:

Conditioned on $\tau_{i,j}$, $h_{i,j}$ is a complex zero-mean circular-symmetric Gaussian random variable with variance:

$$\sigma_h(\tau_{i,j})^2 \equiv \mathbf{E}[|h_{i,j}|^2 | \tau_{i,j}] = \sigma_h^2 \cdot \exp(-\bar{\tau}_i/\bar{\eta}) \cdot \exp(-\Delta\tau_{i,j}/\eta)$$

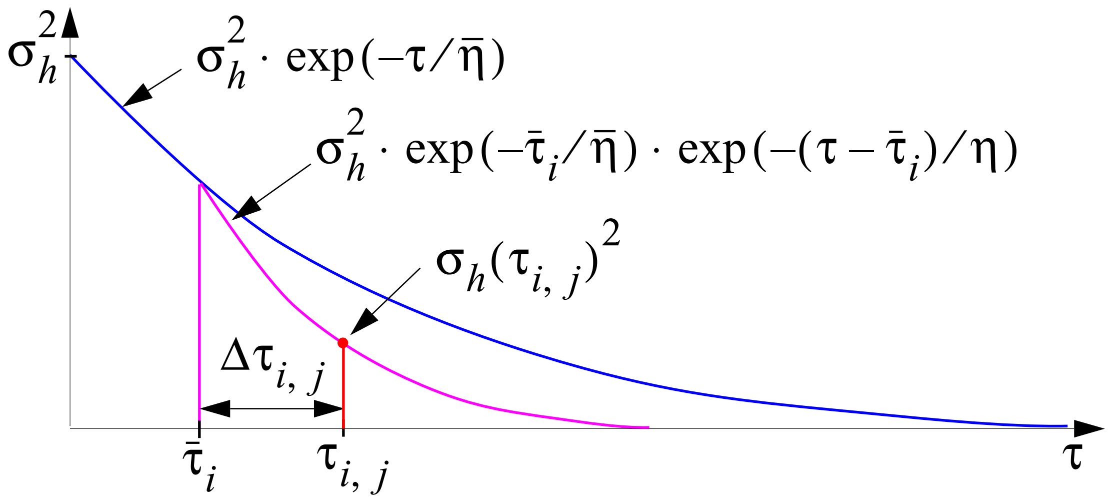

Experimental values for $\bar{\eta}$ and η:

- $\bar{\eta} = 60$ ns
- $\eta = 5 - 10$ ns

WAND model

Include before --- Main characteristics:

Cell type	• Picocell
Area	• Indoor
Application range	• 2, 5, and 17 GHz bands
Time-variant azimuth-delay SFSF	• $g(t;\phi, \tau) \equiv \sum_{i=1}^{N_t} g_i(t)\delta(\phi - \phi_i)\delta(\tau - \tau_i(t))$ $\left(g(t;\tau) = \sum_{i=1}^{N_t} g_i(t)\delta(\tau - \tau_i(t))\right)$
Input	• Area type: small, large rooms, factory halls, corridors • Velocity of the mobile station

WAND model

Local dispersion:

Azimuth-delay spread function:

$$\boxed{h(\phi, \tau) \equiv \sum_{i=1}^{N} h_i \delta(\phi - \phi_i) \delta(\tau - \tau_i)}$$

where

- N is a Poisson distributed random variable.
- $\{\phi_i\}$: sequence of independent, uniformly distributed random azimuths
- $\{\tau_i\}$: sequence of independent, exponentially distributed random delays with common expectation $\mathbf{E}[\tau_i] = \sigma_d$.
- $\{h_i\}$: sequence of independent, zero-mean complex Gaussian random amplitudes with individual variance

$$\mathbf{E}[|h_i|^2 | \phi_i = \phi, \tau_i = \tau] \propto \exp\{-\tau/\sigma_a\}$$

WAND model

Local dispersion (cont'd):

Short term time-variant delay SF:

$$\boxed{g^{(ST)}(t;\tau) \equiv \sum_{i=1}^{N} \underbrace{h_i \exp\{j2\pi\nu_i t\}}_{g_i(t)} \delta(\tau - \tau_i)}$$

with $\nu_i \equiv \frac{v}{\lambda}\cos(\phi_i)$ denoting the Doppler frequency.

WAND model

Local scattering function (cont'd):

Local azimuth-delay scattering function:

$$\boxed{\begin{aligned} P_L(\phi, \tau) &\equiv \mathbf{E}_L[|h(\phi, \tau)|^2] \\ &= \sum_{i=1}^{N} |h_i|^2 \delta(\phi - \phi_i)\delta(\tau - \tau_i) \end{aligned}}$$

Local delay scattering function:

$$\boxed{\begin{aligned} P_L(\tau) &\equiv \mathbf{E}_L[|g^{(ST)}(t;\tau)|^2] \\ &= \sum_{i=1}^{N} |h_i|^2 \delta(\tau - \tau_i) \end{aligned}}$$

WAND model

Global scattering function:

Global azimuth-delay scattering function:

$$\boxed{\begin{aligned} P(\phi, \tau) &\equiv \mathbf{E}[P_L(\phi, \tau)] \\ &\propto \exp\{-\tau/\sigma_\tau\} \end{aligned}}$$

Global delay scattering function:

$$\boxed{\begin{aligned} P(\tau) &\equiv \mathbf{E}[P_L(\tau)] \\ &\propto \exp\{-\tau/\sigma_\tau\} \end{aligned}}$$

with delay spread

$$\boxed{\sigma_\tau = (\sigma_a^{-1} + \sigma_d^{-1})^{-1}}$$

WAND model

Local versus global delay scattering function:

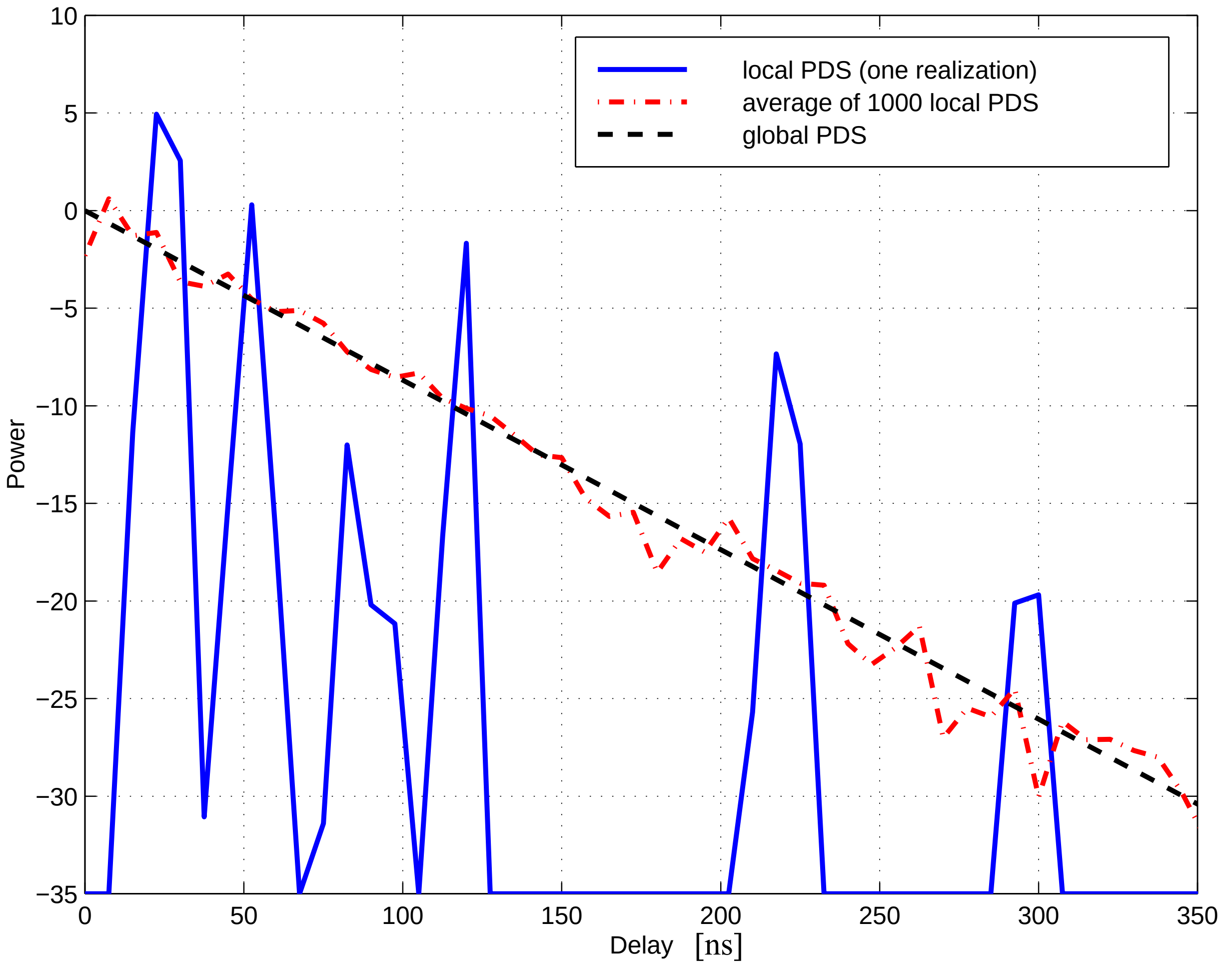

WAND model

Fluctuations of the number of impinging waves:

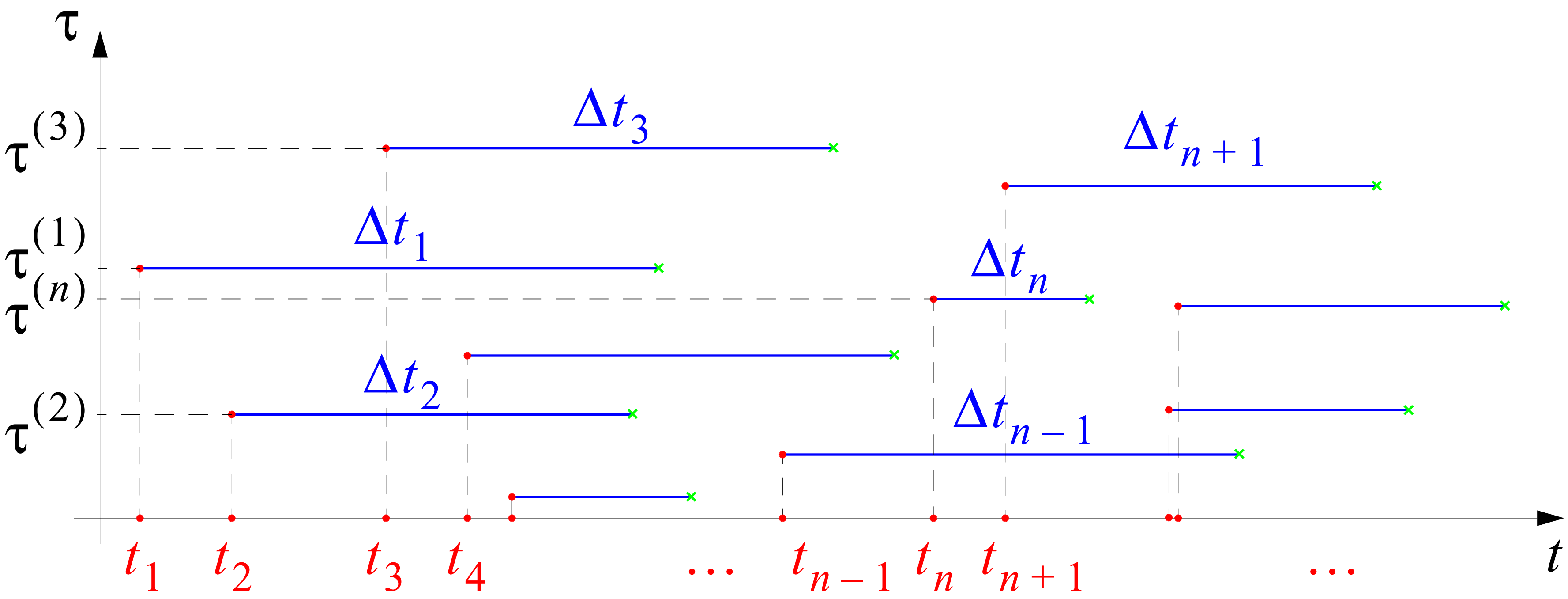

- *Birth times:* $\{t_n\}$: Uniform Poisson process with rate $(\Lambda_b)^{-1}$.
- *Live times:* $\{\Delta t_n\}$: Independent and identically, exponentially distributed random variables with expectation $\mathbf{E}[\Delta t_n] = \Lambda_l$.

WAND model

Fluctuations of the number of impinging waves (cont'd):

Let $N_t \equiv$ number of "active" components in $g(t;\tau)$ at time t.

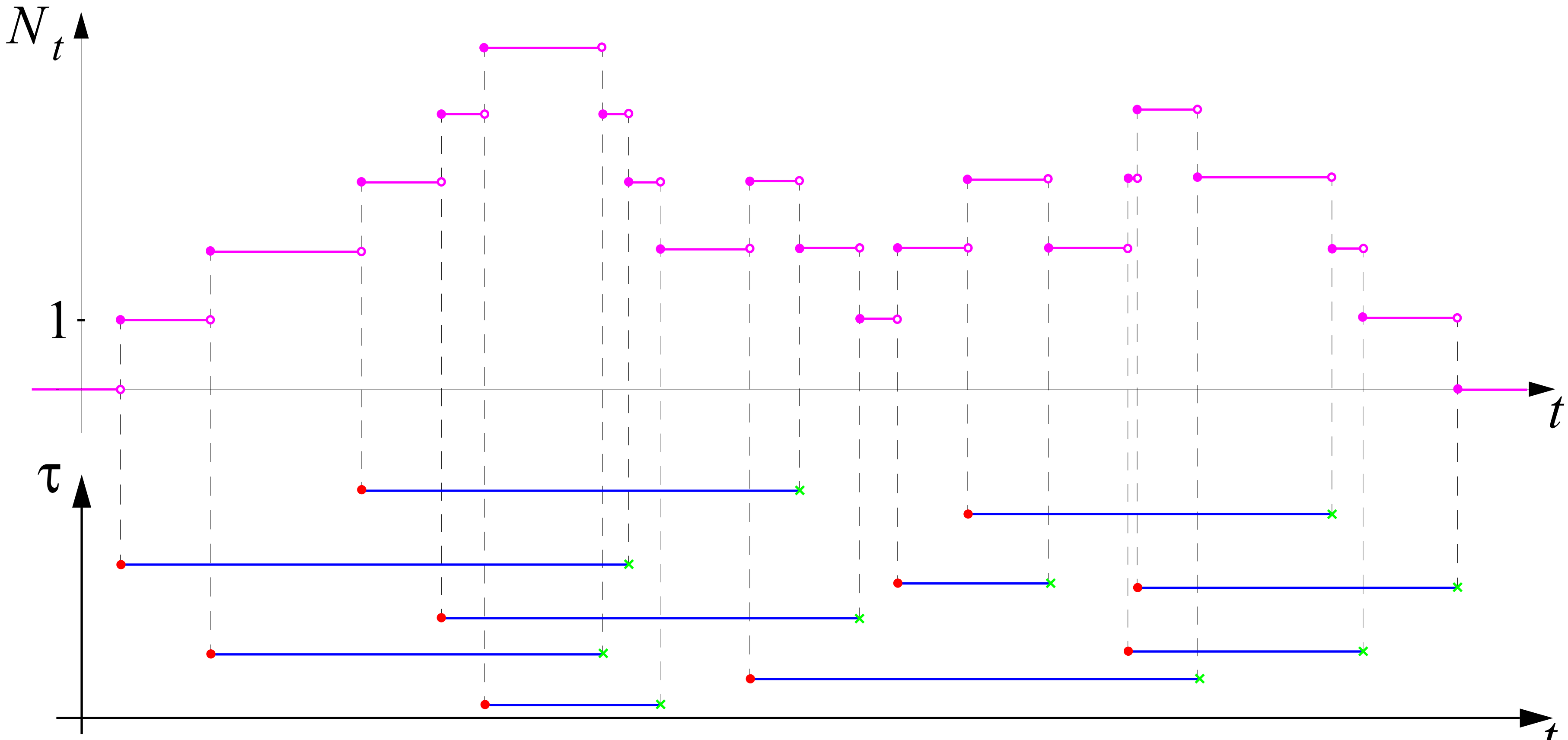

WAND model

Fluctuations of the number of impinging waves (cont'd):

N_t is a Poisson distributed random variable with expectation

$$\boxed{\mathbf{E}[N_t] = \frac{\Lambda_l}{\Lambda_b}}$$

WAND model

Fluctuations of the number of impinging waves (cont'd):

Example of a realization of N_t: $(\mathbf{E}[N_t] = 10)$

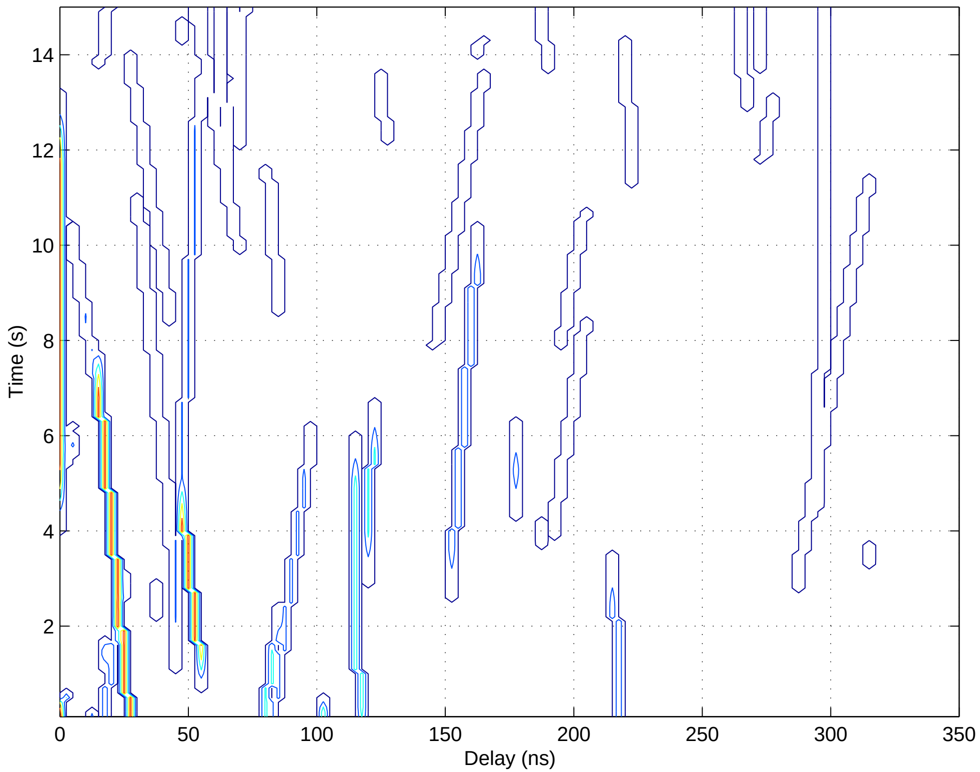

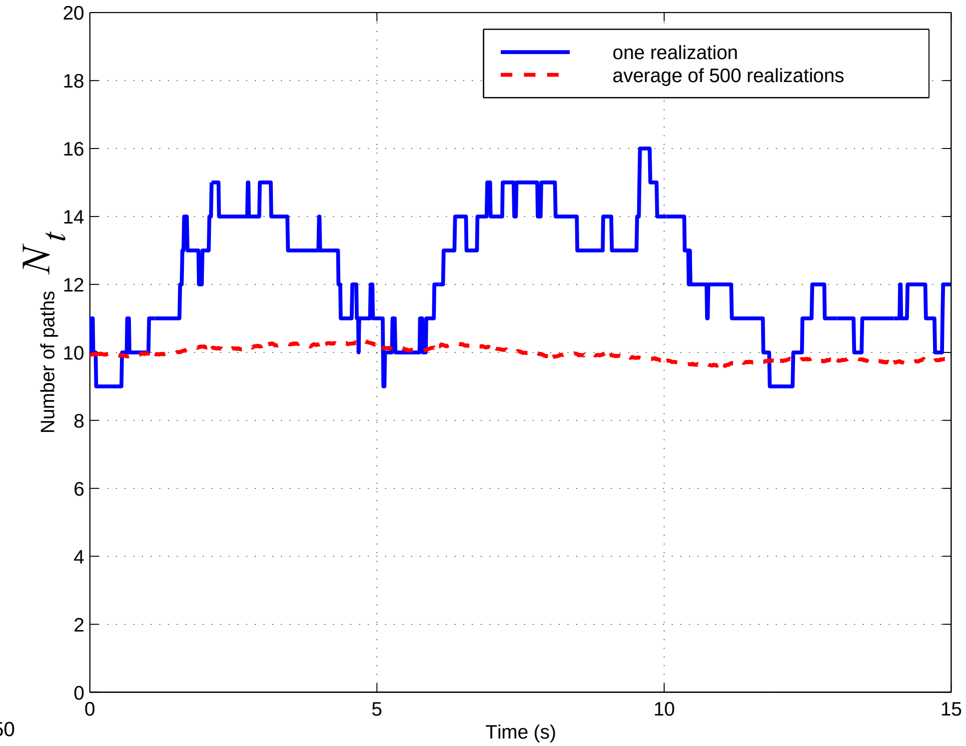

WAND model

Long-term variations of $g_i(t)$ **:**

$$\boxed{g_i(t) \;=\; z_i(t) \cdot g_i^{(\mathrm{ST})}(t)}$$

Transition function:

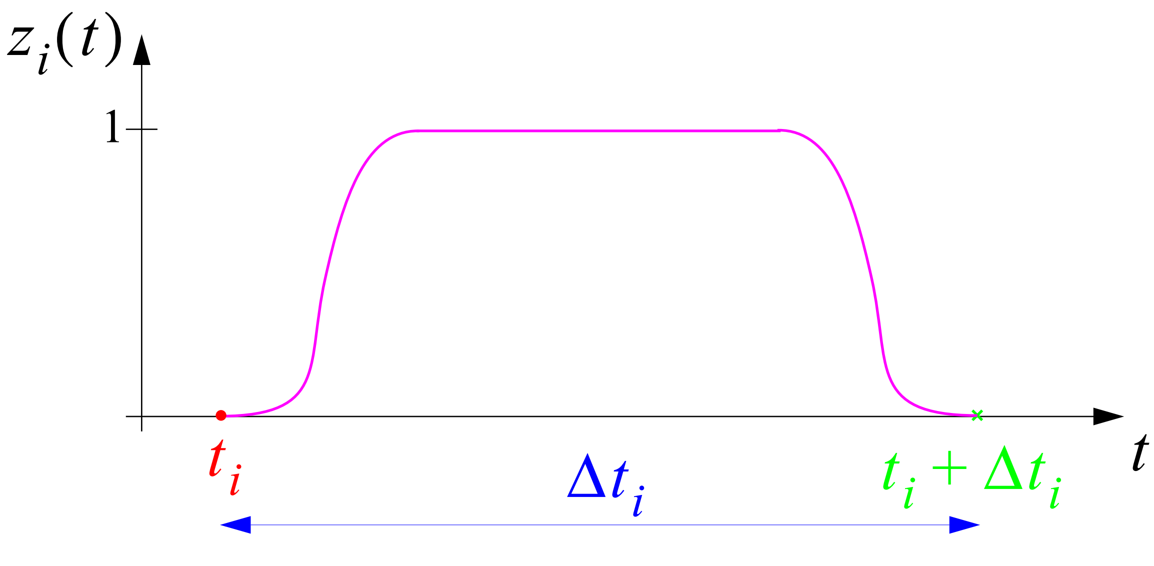

WAND model

Long-term variations of $g_i(t)$ (cont'd):

Selected shape for $z_i(t)$:

$$\boxed{z_i(t) \equiv z\left(\frac{t - t_i}{\Delta t_i}\right)}$$

with the "pattern function"

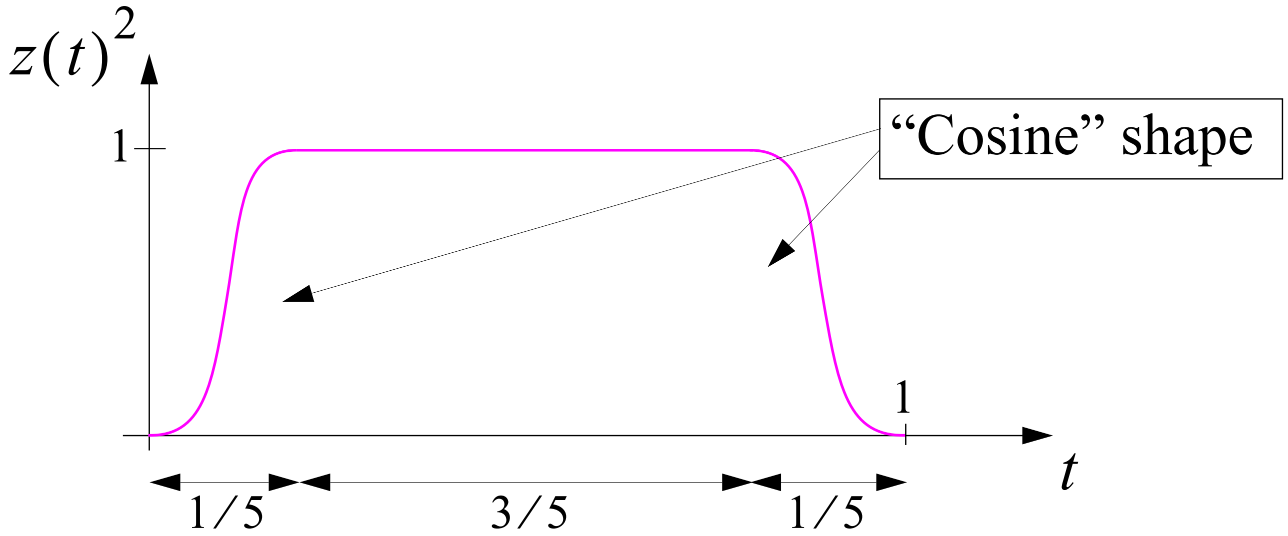

WAND model

Long-term variations of $g_i(t)$ (cont'd):

Example of a realization of the long-term fluctuations of the instantaneous power of the components $g_i(t)$:

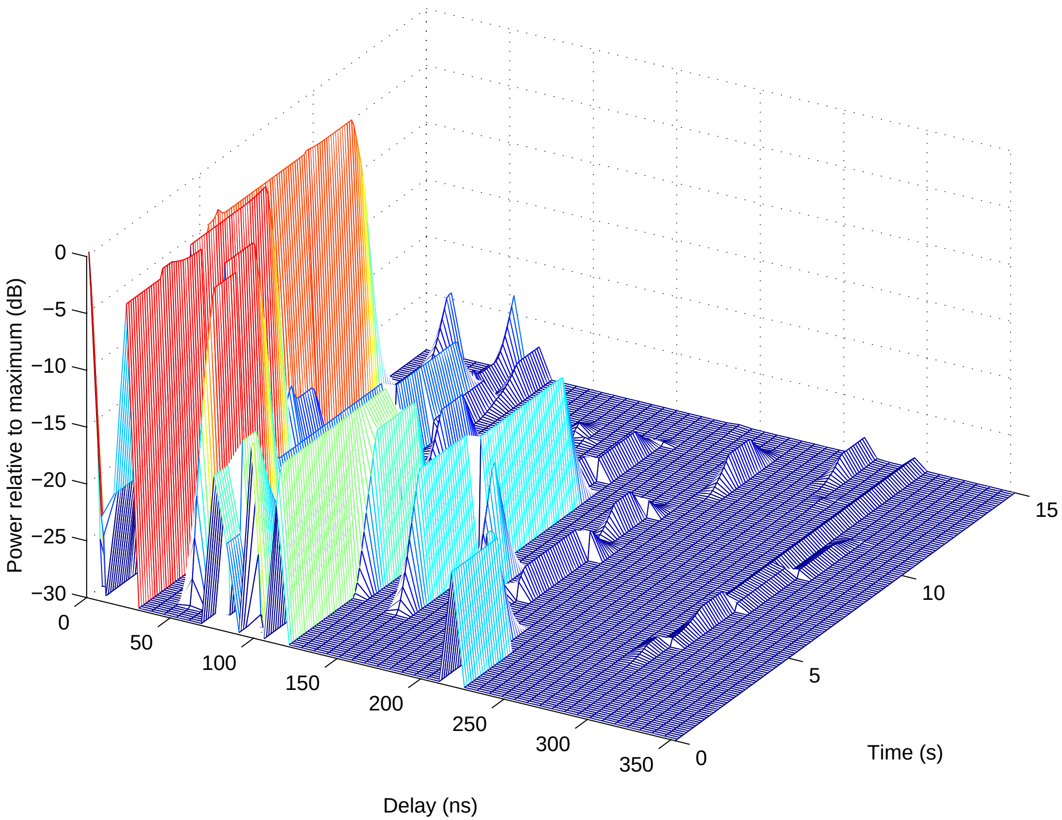

Instantaneous power of $g_i(t)$:

$$z_i(t)^2 |h_i|^2$$

WAND model

Long-term variations of $\tau_i(t)$:

$$\boxed{\tau_i(t) = \tau_i - \frac{\nu_i}{f}[t - (t_i + \Delta t_i/2)]}$$

where $\nu_i = \dfrac{v}{\lambda}\cos(\phi_i)$ is the Doppler shift of the ith component.

WAND model

Long-term variations of $\tau_i(t)$ (cont'd):

Example of a realization of the long-term fluctuations of the relative delays:

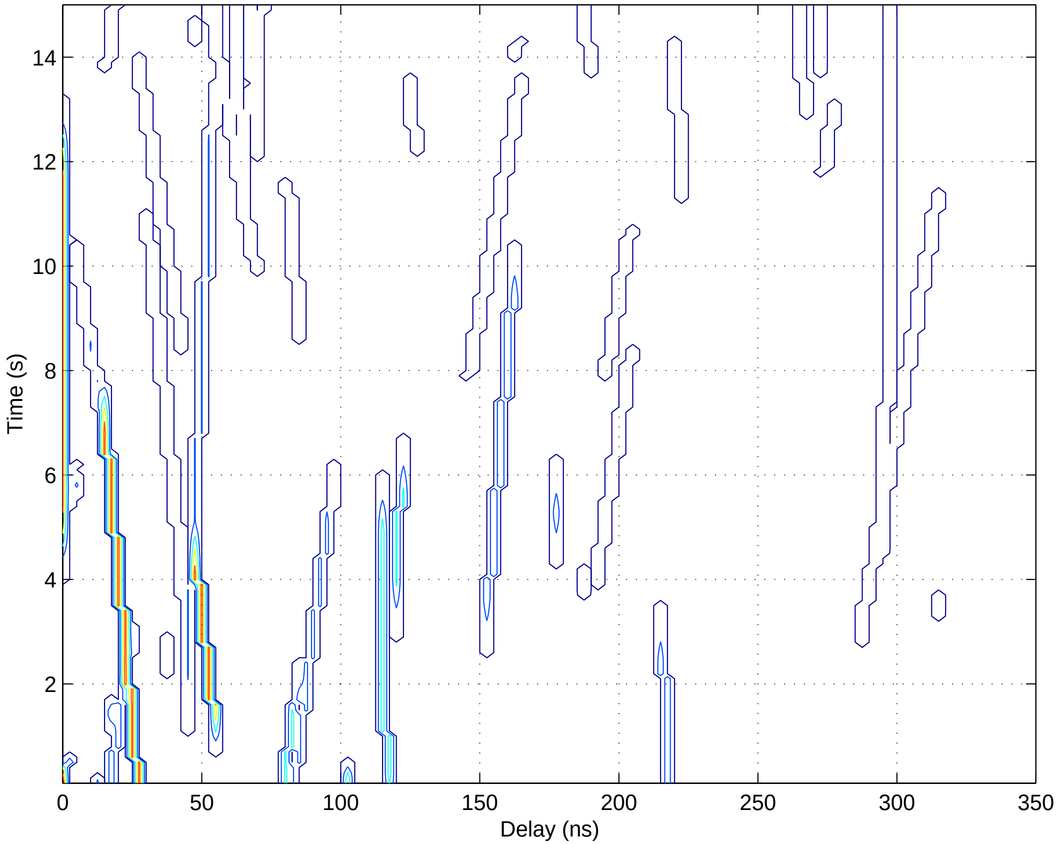

WAND model

Example of a realization of a time-variant delay SF:

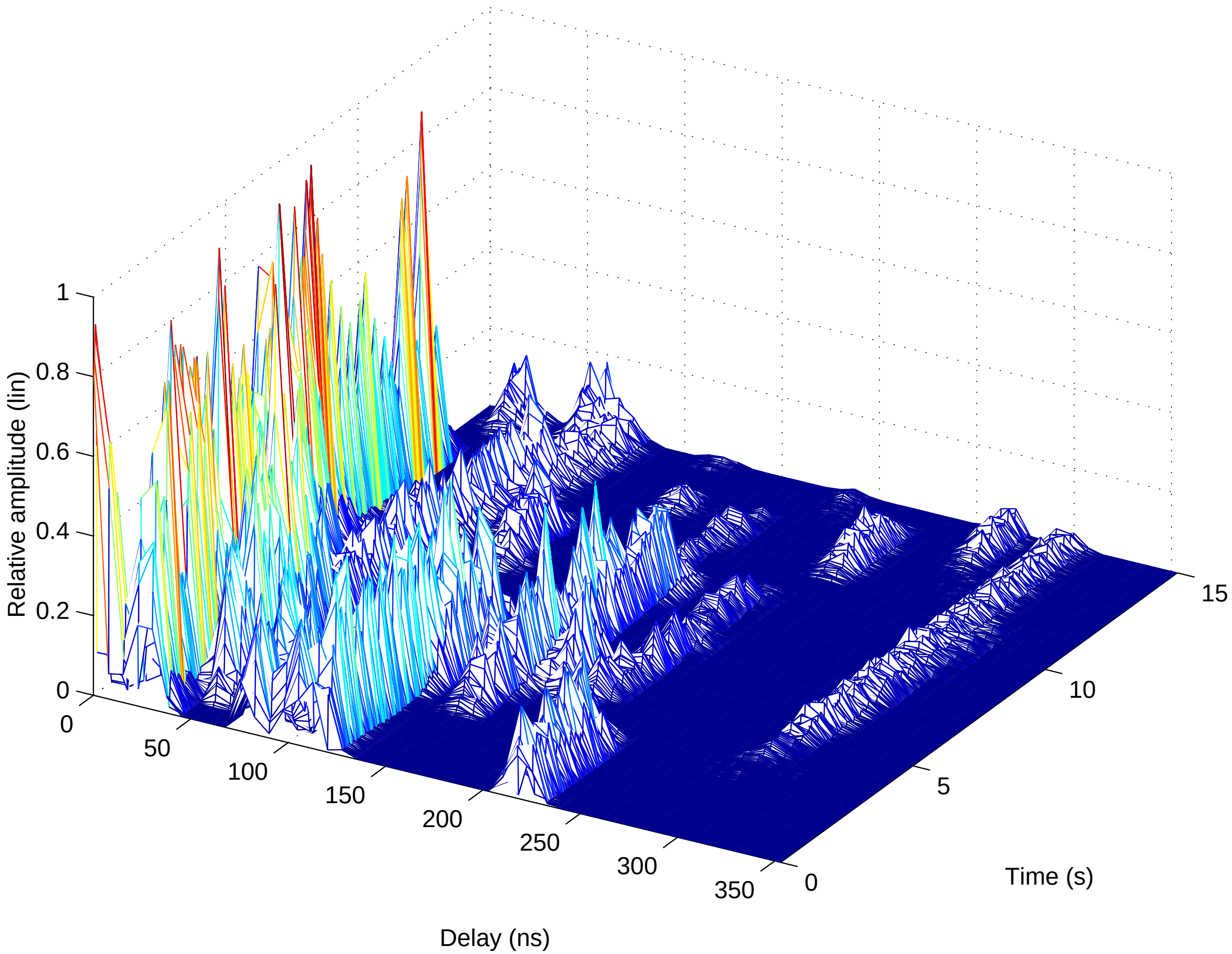

Spencer-Jeffs-Jensen-Swindlehurst Model

Main characteristics:

Cell type	• Picocell
Area	• Indoor
Time-invariant azimuth-delay SF	• $h(\phi, \tau) = \sum_{i=0}^{N} \sum_{j=0}^{J(i)} h_{i,j} \cdot \delta(\phi - \phi_{i,j})\delta(\tau - \tau_{i,j})$ Cluster index Index of the components within the clusters Component azimuth of incidence Component delay
Main features	• Time-invariant • The model is an extension of the model by Saleh-Valenzuela to include dispersion in azimuth of arrival. The concept of double Poisson process is maintained.

Spencer-Jeffs-Jensen-Swindlehurst Model

Stochastic model for $\{\phi_{i,j}\}$**:**

- Cluster delays $\{\bar{\phi}_i\}$: (i) $\bar{\phi}_0 = 0$

  (ii) $\{\bar{\phi}_i; i = 1, 2, \ldots, N\}$: Independent uniformly distributed over $[0, 2\pi)$.

- Delays within cluster i:

  (i) $\phi_{i,j} \equiv \bar{\phi}_i + \Delta\phi_{i,j}$, $j = 0, 1, 2, \ldots, J(i)$, $i = 1, \ldots, N$;

  (ii) $\{\Delta\phi_{i,j}; j = 1, \ldots, J(i)\}$: Independent, Laplace($\sigma_\phi(i)$);

  (iii) $\{\{\Delta\phi_{i,j}; j = 1, \ldots, J(i)\}; i = 1, \ldots, N\}$: independent sets

Spencer-Jeffs-Jensen-Swindlehurst Model

Probability density function of $\Delta\phi_{i,\,j}$ [$\sigma_\phi = 26°$]:

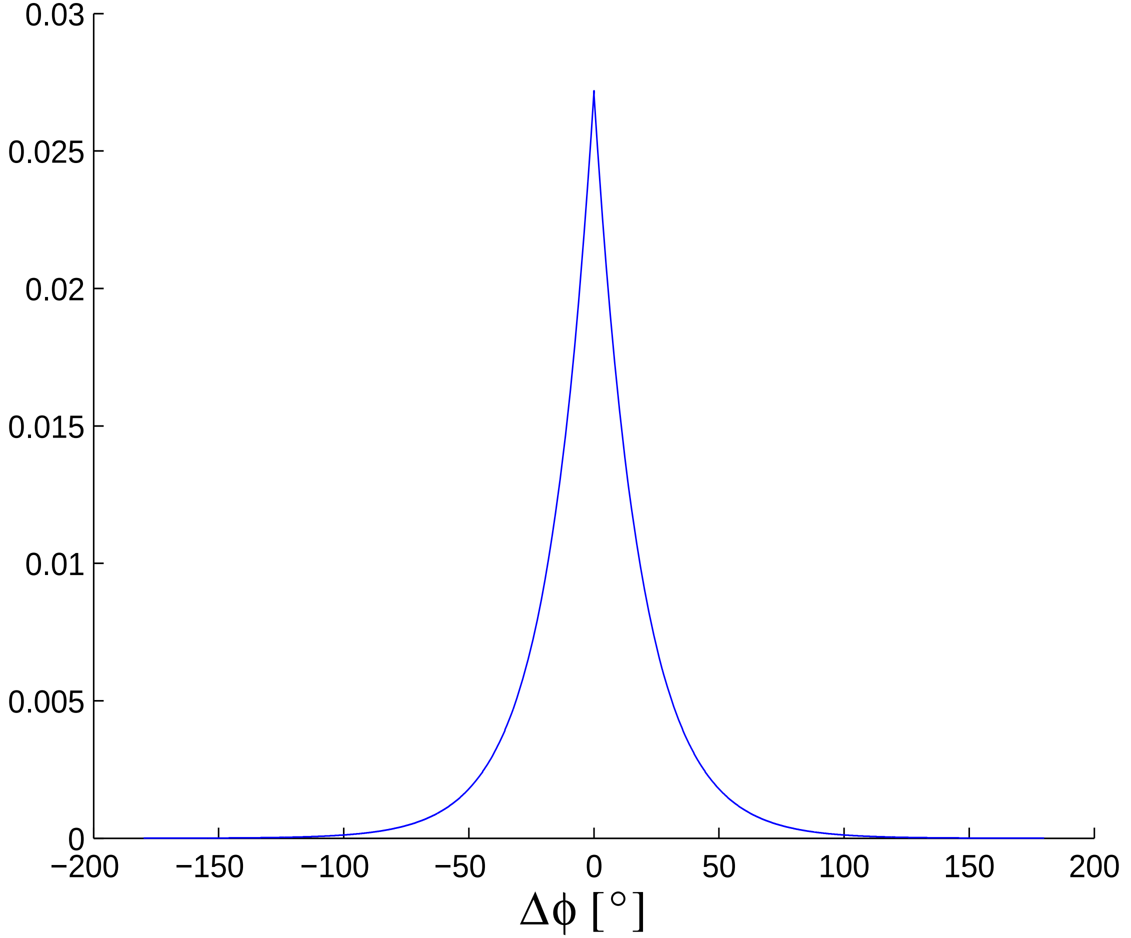

Spencer-Jeffs-Jensen-Swindlehurst Model

Additional independence assumption:

The following three sets of random variables

$$\{\bar{\tau}_i, \Delta\tau_{i,j}; j = 0, 2, \ldots, J(i), i = 1, \ldots, N\}$$

$$\{\bar{\phi}_i; i = 1, \ldots, N\}$$

$$\{\Delta\phi_{i,j}; j = 0, 2, \ldots, J(i), i = 1, \ldots, N\},$$

are independent.

Estimates the model parameters [Building 1, Building 2]:

- $\bar{\eta} = 34\text{ns}, 78\text{ns}$
- $\eta = 29\text{ns}, 82\text{ ns}$
- $1/\Lambda = 17\text{ns}, 17\text{ ns}$
- $1/\lambda = 5\text{ns}, 7\text{ ns}$
- $\sigma_\phi = 26°, 22°$

IEEE 802.11 Model

Main characteristics:

Cell type	• Picocell (indoor and outdoor)
Area	• Model (M) B (delay spread: 15ns): residential LOS/NLOS • M C (30ns): Small office NLOS, typical offices LOS • M D (50ns): Typical office NLOS, large office LOS • M E (100ns): Large office NLOS, large spaces (indoor & outdoor) LOS • M F (150ns): Large space (indoor & outdoor), NLOS
Application range	• 2 and 5 GHz bands
Biazimuth-delay SF	• $h(\phi_1, \phi_2, \tau) = \sum_{i=1}^{N} \sum_{j=1}^{J(i)} h_{i,j}(\phi_1, \phi_2, \tau)$
Input	• Area type • Velocity of the mobile station
Feature	• The model is inspired from the Spencer-Jeffs-Jensen-Swindlehurst model

IEEE 802.11 Model

Stochastic properties of the biazimuth delay SF:

$$h(\phi_1, \phi_2, \tau) = \sum_{i=1}^{N} \sum_{j=1}^{J(i)} h_{i,j}(\phi_1, \phi_2, \tau)$$

- $h_{i,j}(\phi_1, \phi_2, \tau)$: complex uncorrelated process
- $\mathrm{E}[|h_{i,j}(\phi_1, \phi_2, \tau)|^2] = \sigma(\tau_{i,j})^2 f_{\sigma_{\phi_1}(i)}(\phi_1 - \phi_{1,i}) f_{\sigma_{\phi_2}(i)}(\phi_2 - \phi_{2,i}) \cdot$
  $\delta(\tau - \tau_{i,j})$
- $\tau_{i,j} = n_{i,j}\Delta\tau \qquad \Delta\tau = 10\mathrm{ns} \qquad n_{i,j}$ integer
- $f_{\sigma_\phi}(\phi) \propto \exp(-\sqrt{2}|\phi|/\sigma_\phi) \qquad -180 \le \phi < 180$ (Laplace)

IEEE 802.11 Model

Stochastic properties of the biazimuth-delay SF (cont'd):

- The area-dependent parameters $N, \sigma(\tau), \sigma_{\phi_1}(i), \sigma_{\phi_2}(i)\ J(i)$, n_{ij}, $j = 1, 2, \ldots, J(i)$, $i = 1, \ldots, N$ are provided in tables.

Some illustrative figures:

- Number of clusters I: B & C: 2; D: 3, E: 4; F: 6
- Azimuth spread (departure) σ_{ϕ_1}: 14.4-55.2 deg
- Azimuth spread (incidence) σ_{ϕ_2}: 14.4-55.0 deg
- Number of paths/cluster J:

  Cluster 1: 5-16; Cl. 2: 7-12; Cl. 3: 4-7; Cl. 4: 3-4; Cl. 5 & 6: 2

Comment:

The Kronecker factorization applies to the proposed MIMO (narrow-band) transfer matrix, which is inconsistent with the above model

3GPP SCM

Main characteristics:

Cell type	• Macrocell (BS-BS spacing 3km), Microcell (< 1 km)
Area	• Urban macro- (U-Ma) and microcell (U-Mi), suburban macrocell (S-Ma)
Frequency range	• 2 GHz-band
Biazimuth-Doppler-delay SF	• $h(\phi_1, \phi_2, \upsilon, \tau) = \sum_{n=1}^{N} h_n(\phi_1, \phi_2, \upsilon, \tau)$ Cluster index $h_n(\phi_1, \phi_2, \upsilon, \tau) =$ Subpath index $= \sqrt{\frac{P_n \gamma_s}{M}} \sum_{m=1}^{M} \sqrt{G_1(\phi_{1,n,m})} \sqrt{G_2(\phi_{2,n,m})} \exp(j2\vartheta_{n,m})\mathrm{x}$ $\delta(\phi_1 - \phi_{1,n,m})\delta(\phi_2 - \phi_{2,n,m})\delta(\nu - \nu_{n,m})\delta(\tau - \tau_{n,m})$ $\nu_{n,m} = \frac{\lVert\vec{v}\rVert}{\lambda}\cos(\phi_{2,n,m} - \phi_{\vec{v}})$

3GPP SCM

Main features	• $N = 6$ clusters • Uplink-downlink reciprocity • Site-to-site correlated shadowing with 0.5 correlation coefficient • Further options: - Per-path polarization - "Bad urban" scenario with 5th and 6th paths allocated as "far" clusters - LOS scenario (microcell only) specified by a K-factor: $K(d) = 13 - 0.03d$ [dB] (d: distance base station - mobile station) - Urban canyon (modification of the angles of arrival)

3GPP SCM

Characteristics of "one-bounce" clusters:

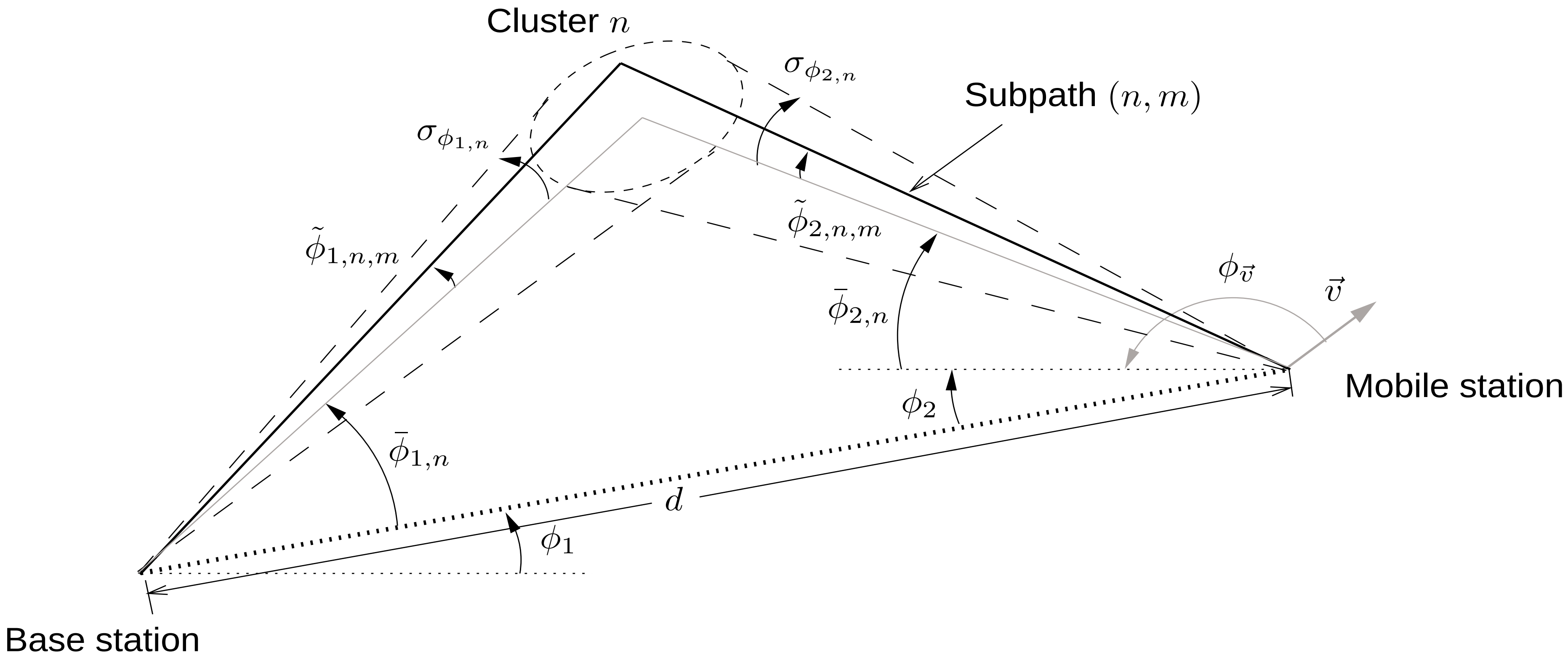

3GPP SCM

Parameters:

Environment parameters:

- Distance BS-MS d and azimuths ϕ_1, ϕ_2 from one station to the other [determined from the cell layout]
- MS velocity direction: $\phi_{\vec{v}}$ uniformly distributed over $[0, 2\pi)$

Path loss and shadowing

- Path loss:
  - Macrocell: Hata model
  - Microcell: COST231-Walfish-Ikegami model
- Shadowing γ_s:
  - Macrocell: $10\log(\gamma_s) \sim \mathrm{Gauss}(0, \varsigma_{\gamma_s}{}^2)$, with $\varsigma_{\gamma_s} = 8[\mathrm{dB}]$
  - Microcell: $10\log(\gamma_s) = 4\mathrm{dB}$ (LOS); $10\mathrm{dB}$ (NLOS)

3GPP SCM

"Global" spread factors:

- Delay spread:

  $E[\sigma_\tau]$: S-Ma: 170ns; U-Ma: 650ns; U-Mi: 251ns

  Macrocell:

  $\log(\sigma_\tau) \sim \mathrm{Gauss}(\mu_\tau, \varsigma_\tau^2)$

  - Suburban: $\mu_\tau = -6.80$, $\varsigma_\tau = 0.288$
  - Urban: $\mu_\tau = -6.18$, $\varsigma_\tau = 0.180$

3GPP SCM

"Global" spread factors (cont'd):

- Azimuth spread at BS site

  $E[\sigma_{\phi_1}]$: S-Ma: 5°; U-Ma: 8°, 15°; U-Mi: 19°

  Macrocell:

  $\log(\sigma_{\phi_1}) \sim \mathrm{Gauss}(\mu_{\phi_1}, \varsigma_{\phi_1}^2)$

  - Suburban: $\mu_{\phi_1} = 0.69$, $\varsigma_{\phi_1} = 0.13$
  - Urban, $E[\sigma_{\phi_1}] = 8°$: $\mu_{\phi_1} = 0.81$, $\varsigma_{\phi_1} = 0.34$
  - Urban, $E[\sigma_{\phi_1}] = 15°$: $\mu_{\phi_1} = 1.18$, $\varsigma_{\phi_1} = 0.21$

- Azimuth spread at MS site:

  $E[\sigma_{\phi_2}] = 68°$ (all areas)

3GPP SCM

Correlation between the log-"Global"-factors in macrocells:

- Intrasite correlation coefficients:
  - $\log(\sigma_\tau)$ and $\log(\sigma_{\phi_1})$: +0.5
  - $10\log(\gamma_s)$ and $\log(\sigma_{\phi_1})$: -0.6
  - $10\log(\gamma_s)$ and $\log(\sigma_\tau)$: -0.6
- Intersite correlation of shadowing: 0.5 correlation coefficient
- The four above quantities are random with a joint Gaussian law specified by
  - their expectations $\mu_\tau, \mu_{\phi_1}, \mu_{\gamma_s} = 0$
  - their variances $\varsigma_\tau^2, \varsigma_{\phi_1}^2, \varsigma_{\gamma_s}^2$
  - their correlation coefficients as above specified
  - non-specified correlation coefficients are zero

3GPP SCM

Clustering:

- Number of clusters: $N = 6$
- Number of subpaths per cluster: $M = 20$

Path weights:

- Unnormalized mean-squared weights:

  $P_n = \exp(-\tau_n / \sigma_\tau) 10^{\xi_n / 10}$ $\xi_n \sim \text{Gaussian}(1, 3^2)$ (lognormal per-path shadowing)
- Normalized mean-squared weights: $P_n = P'_n / \sum P'_{n'}$

3GPP SCM

Path delays:

- Macrocell
  - $\tau'_1, \tau'_2, \ldots, \tau'_N \sim \mathrm{Exp}(\sigma'_\tau)$, independent, with $\sigma'_\tau = \eta_\tau \sigma_\tau$
  - $\eta_\tau = 1.4$ (S-Ma); 1.7 (U-Ma)
- Microcell
  - $\tau'_1, \tau'_2, \ldots, \tau'_N \sim \mathrm{Uniform}([0, 1.2]\mu s)$, independent
- $\tau'_{(1)} \geq \tau'_{(2)} \geq \ldots \geq \tau'_{(N)}$ (ordering)
- $\tau_n = \tau'_{(n)} - \tau'_{(1)}, n = 1, \ldots, N$

Subpath characteristics:

- Phases: $\vartheta_{n,m} \sim \mathrm{Uniform}([0, 2\pi))$
- Azimuths of departure $\tilde{\phi}_{1,n,m}$ and of incidence $\tilde{\phi}_{2,n,m}$: Fixed, tabulated.

3GPP SCM

Azimuth dispersion at the BS:

•Per-path nominal azimuth:

-Macrocell:

$$\bar{\phi}_{1,n} \sim \text{Gauss}(0, \sigma_{\bar{\phi}_1}^{\;2}) \text{ with } \sigma_{\bar{\phi}_1} = \eta_{\phi_1}\sigma_{\phi_1}$$

- Suburban: $\eta_{\phi_1} = 1.2$
- Urban: $\eta_{\phi_1} = 1.3$

- Microcell:

$$\bar{\phi}_{1,n} \sim \text{Uniform}(-40°, 40°)$$

•Per-path azimuth spread:

- Macrocell: $\sigma_{\phi_{1,n}} = 2°$
- Microcell: $\sigma_{\phi_{1,n}} = 5°$

3GPP SCM

Azimuth dispersion at the MS:

- Per-path nominal azimuth:

$$\bar{\phi}_{2,n} \sim \mathrm{Gauss}(0, \sigma_{\bar{\phi}_{2,n}}^{2})$$

The per-path azimuth spread $\sigma_{\bar{\phi}_{2,n}}$ is a monotone increasing function of the path weight:

$$\sigma_{\bar{\phi}_{2,n}} = 104.12(1 - \exp(-0.2175|10\log(P_n)|))$$

- Per-path azimuth spread:

$$\sigma_{\phi_{2,n}} = 35° \text{ (all areas)}$$